Scanning Microscopy

Volume 10 | Number 4 Article 13

1-22-1996

The Role of Defects in Semiconductor Materials and Devices

D. B. Holt
Imperial College of Science, Technology and Medicine, d.b.holt@ic.ac.uk

Scanning Microscopy, Vol. 10, No. 4, 1996 (Pages 1047-1078) 0891-7035/96$5.00+.25
Scanning Microscopy International, Chicago (AMF O'Hare), IL 60666 USA

THE ROLE OF DEFECTS IN SEMICONDUCTOR MATERIALS AND DEVICES

D.B. Holt

Department of Materials, Imperial College of Science, Technology and Medicine,
London SW7 2BP, U.K.

Telephone number: +44-171-5895111 / FAX number: +44-171-5843194 / E.mail: d.b.holt@ic.ac.uk

(Received for publication September 14, 1994, and in revised form January 22, 1996)

Abstract

This literature review leads to the conclusion that recently the basis for an understanding of the electrical and optical properties of structural defects in semiconductors, especially in silicon, has begun to emerge. This is due largely to the ability of scanning electron microscopy (SEM) electron beam induced current (EBIC) and cathodoluminescence (CL) to determine the properties of single, well-defined defects in "state of the art" material. However, there are still major differences concerning the physical models to be used to explain different forms of dislocation EBIC contrast variation with temperature and beam current. Basic ideas in this field are emphasized. In contrast, there has been little systematic fundamental study of the role of defects in devices. Well-known correlations of properties with dislocation densities show that defects in materials and devices are undesirable, although the numbers that can be tolerated are often large and vary greatly from one material to another. Proposals to exploit defects in devices have not been adopted in practice. The few particular cases of the physical mechanisms of the influence of defects on device performance that have been studied are outlined. The role of defects in devices is ripe for the application of scanning beam techniques.

Key Words: Dislocations, electrical effects, impurity decoration, devices, yield, failure.

Introduction

The production of large crystals of germanium of purity and perfection vastly better than any previously known, by the development of Czochralski crystal pulling and the invention of zone refining, was necessary to make possible the first discrete-device solid state electronics. Similar developments for silicon, plus the invention of planar technology, made possible integrated-circuit (IC) microelectronics and the evolution of highly controlled epitaxial multi-layer growth techniques for III-V compounds and alloys enabled optoelectronics (photonics) to emerge.

Correlations of defect density with properties and early dislocation studies

It was soon found that improvements in properties important for device operation correlated with falling defect densities in the early Ge crystals. For example, the minority carrier lifetime in germanium at room temperature increases with decreases of the dislocation density as shown in Figure 1 (Wertheim and Pearson, 1957). This indicates that dislocations act as traps or recombination centers. Conversely, it was found that so-called 1/f electrical noise was orders of magnitude greater in germanium after plastic deformation (Brophy, 1956, 1959). The fact that dislocations increase device noise shows that they act as generation-recombination centers (Morrison, 1956; for a review of these early studies, see Bardsley, 1960). Hence, the dislocation density was used as the basic parameter for monitoring the quality of the materials produced. The discovery of these defect correlations led to much of the classic research on the crystallography, origin and properties of dislocations being done at the great American industrial electronics laboratories in the late 1940s and 1950s.

Dislocation density correlations are still important in evaluating new materials and device technologies. Recently, high-efficiency (3.8%), bright, long-lived blue light emitting diodes (LEDs) were announced by a Japanese firm (Nichia Chemical Company) using GaN grown on sapphire. These emit 1 mW of light peaked at 450

List of Symbols Used

$\mathbf{b}$ ≡ the Burgers vector (b is its magnitude)
C_e ≡ the probability of an electron jumping to or from a dislocation state
D ≡ the minority carrier diffusion coefficient
D_h ≡ D in n-type material
E_C ≡ the conduction band edge (lowest energy level)
E_d ≡ the energy of the dislocation trap state in the charge-controlled recombination model
E_t ≡ the energy of the trap/recombination centers of dislocations in the SRH recombination model
E_V ≡ the energy of the highest valence band state
f ≡ fraction of dislocation traps occupied by an electron
I_b ≡ the current in the beam of an SEM
J ≡ the dislocation recombination current per unit length
J_e ≡ the net rate of electron capture per unit length of dislocation
J_h ≡ the rate of hole capture per unit length of dislocation
J_i ≡ the rate of electron entry into the dislocation states from the conduction band
k ≡ the Boltzmann constant
n ≡ the electron density
n_i ≡ the intrinsic carrier concentration
n_1 ≡ the electron concentration in equilibrium with the dislocation trap states
n_o ≡ the equilibrium electron density in the absence of dislocations
N_C ≡ the density of states in the conduction band
N_D ≡ the density of donor atoms
N_d ≡ the number of recombination states per unit of dislocation length
N_t ≡ the concentration of traps
N_v ≡ the density of states in the valence band
p ≡ the concentration of holes
p_1 ≡ the hole concentration in equilibrium with the dislocation trap states
p_o ≡ the equilibrium hole concentration
q ≡ the charge on an electron
Q ≡ the charge per unit length on a dislocation
R ≡ the rate of re-emission of dislocation-trapped electrons to the conduction band
r_d ≡ radius of the space charge cylinder around a charged dislocation (Read); radius of the cylinder of reduced minority carrier lifetime round a dislocation (Donolato, Wilshaw)
T ≡ the temperature (K)
T_m ≡ the melting temperature
U ≡ the net rate of carrier recombination at a dislocation (SRH recombination model)
v_{th} ≡ the thermal velocity of the minority carriers
$\langle v_{th} \rangle_n$ ≡ the average thermal velocity of electrons
$\langle v_{th} \rangle_p$ ≡ the average thermal velocity of holes

Greek Symbols

α ≡ a constant
β ≡ a constant, depending on the SEM operating parameters and the specimen geometry
Δp ≡ the excess density of minority carriers injected by the electron beam
Δn ≡ the concentration of injected electrons (= that of holes)
ϵ ≡ relative permittivity
ϵ_o ≡ the permittivity of free space
γ ≡ the strength (line recombination velocity) of a dislocation
λ_D ≡ the Debye length
ϕ ≡ the potential barrier against electrons entering the dislocation from the conduction band
ϕ_o ≡ the potential barrier against electrons leaving the dislocation level for the conduction band
σ ≡ the capture cross-section of a trap
σ_n ≡ the trap capture cross-section for electrons
σ_p ≡ the trap capture cross-section for holes
ρ ≡ the density of dislocations (total length per unit volume so units of, e.g., cm^{-2})
τ ≡ the minority carrier lifetime in the absence of dislocations
τ' ≡ the reduced lifetime inside the enhanced recombination cylinder round a dislocation
τ_{po} ≡ the minority carrier lifetime for holes
τ_{no} ≡ the minority carrier lifetime for electrons

---

nm when driven at 10 mA. These LEDs were about 100 times brighter than previous commercially available SiC blue LEDs (Cook and Schetzina, 1995). Lester *et al.* (1995) reported that LED efficiency varied with etch pit density (ρ) in the III-V materials previously used to make red and yellow emitting LEDs, as shown in Figure 2. Astonishment was caused by their discovery that the bright, long-lived GaN LEDs had densities of 10^{10} dislocations per cm^{-2}. That is, in the new GaN multilayer LEDs, high efficiency was achieved in material with a threading dislocation density from 4 to 6 orders of magnitude higher than the long established GaP and GaAs based materials could tolerate! Lester *et al.* (1995) suggested that this is because GaN is more ionically bonded, so the dislocations are less efficient as non-radiative recombination sites. This illustrates the general finding that there is, for any given device-technology-material combination, some dislocation density "threshold" value, ρ_{crit}. Provided $\rho < \rho_{crit}$, the yield of working devices is satisfactory. Etch pit densities

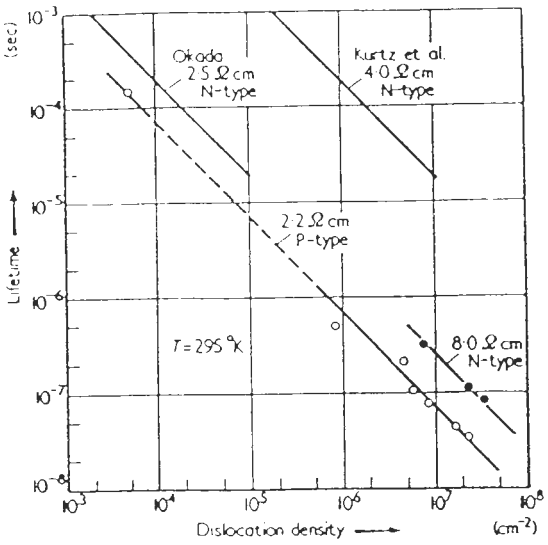

Figure 1. Minority carrier lifetime versus dislocation density in germanium at room temperature (after Wertheim and Pearson 1957).

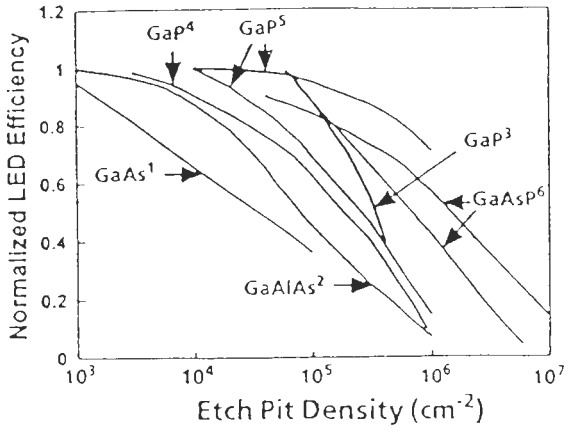

Figure 2. Variation of LED efficiency with dislocation density for devices made with the established III-V materials (the numbers on the figure are the references for the original data in Lester *et al.*, 1995 whence this Figure was taken).

(EPDs), i.e., dislocation densities, are still routinely measured to monitor the quality of Si wafers, and for most purposes, EPDs below 10^4 cm^{-2} are adequate and zero EPD wafers are not needed. Thus, devices can often operate satisfactorily despite the presence of large numbers of defects like the GaN blue LEDs mentioned above. Also, unfortunately (fortunately from the practical point of view) many problems "go away" as the

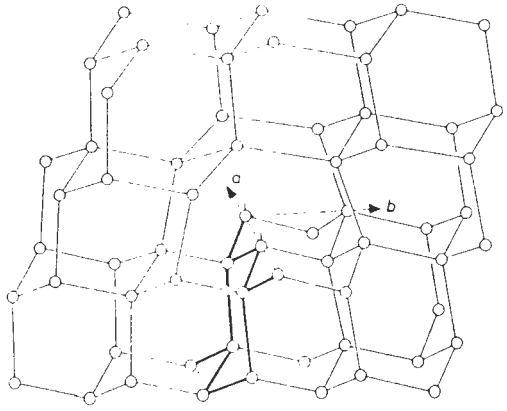

Figure 3. Dangling bonds in the core of an undissociated "shuffle set" 60° dislocation core (after Shockley 1953).

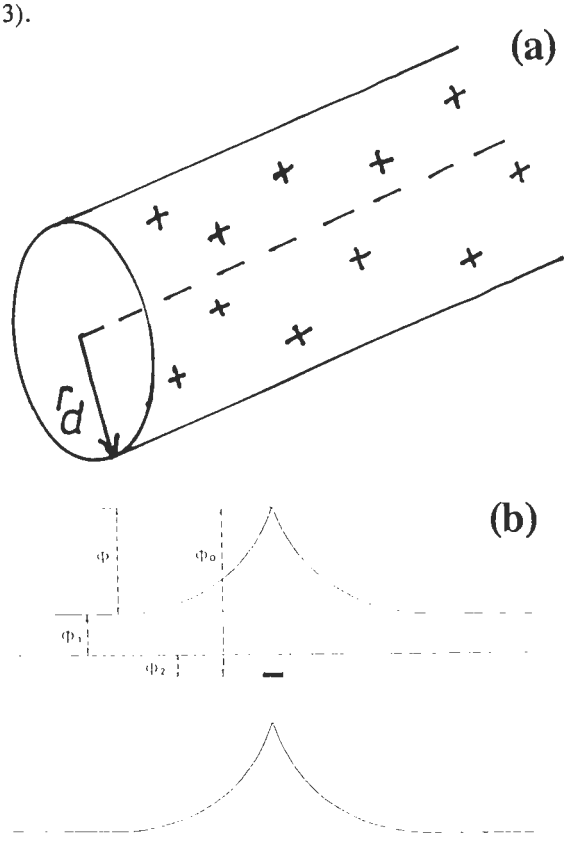

Figure 4. (a) The Read model of charged dislocation line and surrounding space charge cylinder (depletion region). (b) The band bending resulting from the model. (After Wilshaw and Fell 1989.)

---

result of "good housekeeping," i.e., adoption of the best practice based on experience, in the mature Si industry without the problems ever being solved. If the problems do not go away speedily, the process or device will often be abandoned for some competitive process or de-

vice. Hence, industry lost much of its interest in dislocation theory, so only a few examples of the influence of defects on devices have been thoroughly investigated.

Basic semiconductor defect research was then left as a mainly academic, but very active, field (see, e.g., the proceedings of the latest in each of six regular series of conferences in this field listed as part of **Appendix I**).

Early studies concerned the electrical properties of plastically deformed material since this often occurred in processing in the early days with disastrous effects on device yields. Plastically deformed material contains vast numbers of dislocations of various types, in complex configurations, plus the point defect and dipole debris left behind on the slip planes. Agreement between theory and experimental results was difficult to achieve even with complex models, as we will see. Scanning beam methods, especially scanning electron microscopy (SEM) electron beam induced current (EBIC) and cathodoluminescence (CL), and infrared beam induced current (IRBIC), proved capable of the determination of the properties of individual spatially resolved dislocations. This is leading to the achievement of a more satisfactory understanding of the electrical and optical properties of dislocations (and grain boundaries) as a brief literature review below will attempt to show. However, despite the obvious practical importance of the "effects of defects" in devices, surprisingly few cases have been thoroughly investigated. The influence of defects on the operating parameters of devices has not even been reviewed systematically to the author's knowledge so it seemed useful to bring together the research that has been done and to point out the need for further study.

The Earlier Work on the Electrical and Optical Properties of Defects

Why do dislocations have electrical and optical effects?

Shockley (1953) first suggested that in tetrahedrally bonded semiconductors, there would be "dangling bonds" (covalent bonding orbitals that do not reach and bond to a second atom) in the core of dislocations with an edge component. These were then thought to have unit "shuffle set" forms like the 60° dislocation of Figure 3. The dangling bonds would be occupied by only one electron in an intrinsic crystal at low temperatures. The wave functions of adjacent dangling sp^3 hybrid orbitals, he suggested, would overlap to form a half-filled band. The dangling bond energy levels should fall about midway between the bonding states corresponding to the valence band and the covalent antibonding states corresponding to the conduction band.

Such deep dislocation states are the probable main cause of the electrical effects of (relatively) clean dislocations. The unpaired spins of the electrons they contain should be detectable by electron spin resonance (ESR, also known as electron paramagnetic resonance, EPR). Such ESR signals were detected in Si deformed at low temperatures (Alexander *et al.*, 1965; Grazhulis, 1979). For a recent review, see Alexander (1991). However, there are orders of magnitude fewer of these unpaired electrons than the one dangling bond per atomic plane (Fig. 3) along the line of 60° dislocations of the original Shockley model (Weber and Alexander, 1979) although this result was not universally agreed (see, e.g., Kveder *et al.*, 1982). The relatively low density of states per unit length of dislocation, N_d, was explained by crystallographic models showing how rearrangement could eliminate large numbers of dangling bonds in dislocation cores (Hornstra, 1958) and so reduce the energy. It is now believed that dislocations are generally of dissociated glide set form and that the bonds are rearranged to minimize the energy which reduces the numbers of trap states (see the discussion of Hirsch, 1985, and the calculations of Marklund, 1979, and, for a recent review, Duesbury and Richardson, 1991). It was also found that impurities and dislocation cores could interact to alter, passivate or create dislocation states (see, e.g., the references and calculations of Heggie *et al.*, 1989 and Jones *et al.*, 1993, and the recent experimental results to be reviewed below). It is, therefore, now thought that dangling bonds only occur at occasional "special sites" along dislocation lines (Hirsch, 1981, 1985). One hypothesis is that these correspond to kinks in partial dislocations. The detail in ESR signals led to the conclusion that major effects were also due to what are probably point defects such as vacancies or divacancies left as debris behind the moving dislocations and this conclusion is supported by DLTS (deep level trap spectroscopy) results, as we will see below.

It was originally puzzling, since dislocations were expected to have partially filled defect bands of states near the middle of the band gap, that direct current conduction along dislocation lines was not found. It is now believed that partially filled dislocation energy bands do exist but direct current effects are not observed because the lengths along which there are continuous bands are short. Evidence of high frequency alternating current conduction, back and forth along line segments, is observed at low temperatures (Ossipiyan, 1981). These data lead to the conclusion that there is conduction along dislocation lines for lengths corresponding to a few to about 20 dangling bonds in communication. Changes of line direction, kinks, jogs, decorating impurity atoms and nodes joining dislocations into networks could cause breaks between such conducting segments.

In addition to the deep dislocation bands of states believed to arise from dangling bonds and/or impurity decoration, shallow states are believed to arise from the deformation-potential effect of the strain fields of dislocations (e.g., Claesson, 1979) or from the rearranged, strained bonds formed to eliminate dangling bonds (e.g., Jones, 1979).

Recently, it has been found, using photoluminescence spectroscopy, SEM EBIC and CL that the electrical properties of dislocations introduced into silicon as cleanly as possible are usually still dominated by traces of Cu or Ni and this work will be reviewed below.

A possible third source of dislocation electronic properties is the piezoelectric effect. This occurs in adamantine compounds with the sphalerite or wurtzite structures but cannot occur in diamond structure elements because they are centro-symmetric. In the compounds, the elastic strain fields of dislocations produce electric fields (Merten, 1964a,b; Booyens *et al.*, 1977). Booyens *et al.* (1978a,b) also treated some of the effects of piezoelectric dislocations on the conductivity and mobility of III-V materials. Since the piezoelectric coefficients of some of these compounds are large, the resultant effects could be significant but there is no experimental evidence to support this idea at present.

Early Work on the Electrical Effects of Plastic Deformation

In lightly doped n-type Ge it was soon found that very small plastic strains from, e.g., non-uniform cooling known as "quenching strains," sufficed to eliminate the n-type conductivity or even turn the material p-type locally. The Hall mobility was similarly reduced.

The Read theory

Since it was found that dislocations introduced in processing the earliest device material had relatively large effects on n-type conductivity but relatively small effects on p-type Ge, Read (1954a,b) assumed that the deep dangling bond energy states act as acceptors. Therefore, dislocations in n-type Ge have a negative charge, Q, per unit length which is screened by an equal positive space charge in a surrounding volume of radius r_d (Fig. 4a). The spacing of dangling bonds along a 60° dislocation of the form shown in Figure 3 is the spacing of neighbouring atoms in a <110> direction = b, the Burgers vector (b is its magnitude). The line charge is the number of dangling bonds per unit length times the occupation function, f (fraction occupied by a second electron). Hence, for unit length of such a 60° dislocation, we can write, equating the positive space charge to the negative line charge:

$$Q = \pi r_d^2 \, q \, N_D = q \, f/b \qquad (1)$$

where q is the charge on an electron, r_d is the radius of the space charge cylinder and N_D is the donor density. This results in energy band bending as shown in Figure 4b.

In Ge, b = 0.397 nm, so there would be 1/b = 2.5 x 10^7 dangling bonds per cm of such a dislocation. For a dislocation density of 10^9 cm^{-2}, there would be, therefore, 2.5 x 10^{16} dangling bonds per cm^3. At room temperature, Read's various treatments of the statistical problem of the occupation of dislocation states indicated that about one bond in ten would be occupied by a second electron. Thus, a density of 10^9 60° dislocations cm^{-2} would accept 2.5 x 10^{15} electrons per cm^3. This is greater than the total number of charge carriers in 1.7 ohm cm n-type Ge. Experimentally, plastic deformation of the order of a percent, introducing such dislocation densities as this, did turn such lightly doped n-type Ge intrinsic or even p-type.

To relate the theory to the electrical transport properties of deformed Ge, Read (1955) treated the scattering of electrons by an array of parallel dislocations such as might be introduced by plastic bending. He assumed the electrons to make elastic collisions with impenetrable space charge cylinders round the dislocations.

Substituting the value of N_D for 1.7 ohm cm (for Ge) leads to a value of r_d = 1 μm. This means that all the material becomes intrinsic due to incorporation into the space charge cylinders for a dislocation density of about 10^8 cm^{-2}. (Suppose all the dislocations are parallel, form a square array seen end on, and that the cylinders are in contact. Then, each dislocation occupies an area normal to the lines of (2 μm)^2. The dislocation density is the reciprocal of this = 0.25 x 10^8 cm^{-2}). This value is of the same order as the density found above to be ample to absorb all the free electrons. The large size of the space charge cylinders also accounts for the large charge carrier scattering effects observed at lower densities (Bardsley, 1960).

Experimental tests of the Read theory

To test the theory, measurements were first made on bent crystals of Ge by Logan *et al.* (1959) as this is a well-known method for introducing predominantly parallel edge dislocations of one sign. The test was to deduce the density of dislocations from the observed change in conductivity and Hall mobility, $\rho_{theoret}$, and to compare this with the number found by etch pit count, ρ_{expt}. They were only just "in order of magnitude agreement," i.e., they disagreed by a factor of 8 to 9 with $\rho_{theoret} > \rho_{expt}$. Thus, the electrical effects of dislocations, or more correctly of plastic deformation, are even larger than the Read model suggests, so fewer

dislocations than required by this theory can produce the observed electrical effects.

The result of the work of Logan *et al.* (1959) proved to be characteristic. A large body of careful work on Ge (Broudy, 1963) and InSb (Bell *et al.*, 1966; Bell and Willoughby, 1966, 1970) also resulted in dislocation densities calculated from electrical measurements that were nearly an order of magnitude larger than those found by etch pit counting. However, Read's theory is the simplest first approximation treatment and the concept that dislocations are charged and shielded by space charge is still used.

Later work

Subsequently, a great deal of work was done by academic research groups in Germany (Labusch and Schroter, 1978; Schroter *et al.*, 1980; Alexander, 1986; Alexander and Teichler, 1991). These led Schroter to adopt a model in which the dislocation core gives rise to a deep, half-filled band of defect states. This modification of the Read theory made it more acceptable theoretically and yielded good agreement with experiment over a wider range of materials including p-type Ge and Si and a wider range of phenomena than the earlier theory (for a thorough account of this work, see Labusch and Schroter, 1978).

The Figielski model for the effect of dislocations on photoconductivity

A Polish group carried out a substantial body of work on the effects of recombination at dislocations on the photoconductivity of plastically deformed Ge and Si and its rate of decay. This led Figielski and his coworkers (Figielski, 1978) to introduce the idea (also used by Morrison, 1956, to account for electrical noise) that recombination at dislocations resulted from the capture of electrons and holes at rates limited by the potential energy barrier due to the negative line and surrounding space charges which result in local band bending, as shown in Figure 4b. This led to the Figielski (1978) dynamical model of recombination.

Energy Levels in the Band Gap Due to Plastic Deformation

The conclusions from careful and detailed ESR studies (Alexander, 1991; Weber, 1994) are that: (1) 65% to 80% of the 10^{16} cm^{-3} paramagnetic centers produced by 5% compressive strain of Si at 650°C are point defects or clusters thereof, and (2) dislocations are related to a relatively small number of deep states ($\approx 5 \times 10^{14}$ cm^{-3} for 1% strain) in the middle and upper half of the gap. Thus, apparently, the observed effects of strain on electrical conductivity and Hall mobility are produced predominantly by point defect debris rather than by dislocations. Dislocations also produce shallow states 200 meV or less from the band edges.

Systematic work extending and applying the Read theory led to energy band diagrams for the trap states of dislocations (Schroter *et al.*, 1980). Ossipiyan (1981, 1983) put forward a density of states versus energy band structure for dislocations in silicon on the basis of ESR and microwave low temperature conductivity studies. Combined ESR and DLTS work led to energy band diagrams for dislocations produced by deformation below 0.6 T_m (where T_m is the melting point) as shown in Figures 5a and 5b, and after annealing at or above 0.6 T_m as shown in Figure 5c (Kveder *et al.*, 1982). Levels at depths of 0.24, 0.33 and 0.56 eV were reported by Ono and Sumino (1985). Similar work was reported by Omling *et al.* (1985) and all these groups discussed their differences of interpretation and the role of both dislocation core states and those associated with point defects (which can be eliminated by annealing without reducing the dislocation density).

The Role of Scanning Beam Methods in the Study of the Properties of Defects in Semiconductor Materials

The phenomenological theory of EBIC dark contrast due to Donolato (1978/1979, 1985), with second order corrections by Pasemann (1981), made it possible to determine the strength or recombination velocity of individual defects of any type from scanning beam studies. The strength of a dislocation on the Donolato theory is written as:

$$\gamma = (\pi\, r_d^2) / (D_h \tau') \qquad (2)$$

where D_h is the minority carrier diffusion coefficient in n-type material and τ' is the minority carrier lifetime in the space charge cylinder, reduced compared to the value τ in material far from any dislocation.

This led to extensive EBIC studies of both dislocations (for a review, see Holt, 1989) and grain boundaries. Due to limitations of space, we will not review the work on grain boundaries here. For an introduction to the literature, see the proceedings of the latest in the series of conferences on polycrystalline semiconductors (Strunk *et al.*, 1994; listed in **Appendix I**). For reviews of the scanning beam studies on grain boundaries, see Alexander (1994) and Holt (1994).

Much experimental work was also carried out on dislocation CL contrast by, e.g., Brummer and Schreiber (1974, 1975), and by Hergert and Pasemann (1984). The work of Lohnert and Kubalek (1983),

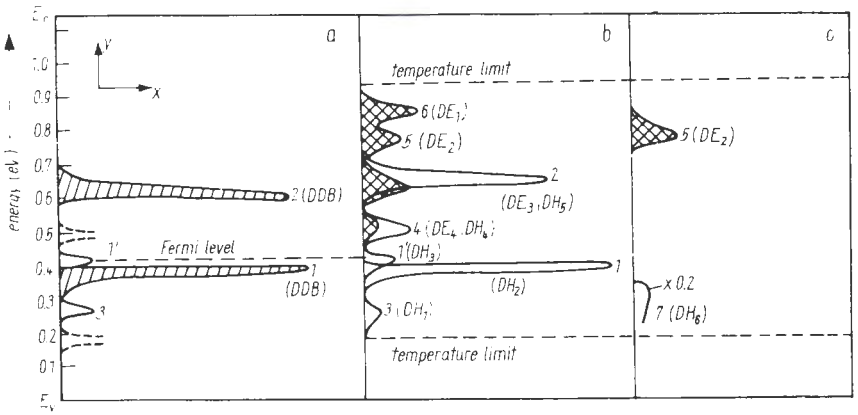

Figure 5. Diagrams of the density of states versus energy for dislocations in Si deformed at temperatures below 0.6 T_m derived from (a) ESR and (b) DLTS and (c) from DLTS data for dislocations annealed at or above 0.6 T_m. For the meanings of the labels on the Figure, see Kveder *et al.* (1982) from whom the Figure is taken.

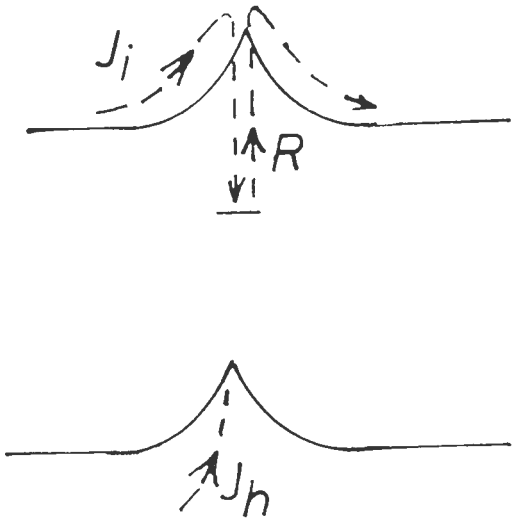

Figure 6. The currents of holes, J_h, and electrons, J_i, flowing into, and the current of electrons re-emitted, R, from a charged dislocation. The net flux of electrons into the dislocation is $J_e = J_i\text{-}R = J_h$ in equilibrium.

Hergert and Pasemann (1984), Pasemann and Hergert (1986), and Jakubowicz (1986) showed that the phenomenological approach could be applied to analyse dark CL contrast.

It is now clear that the importance of SEM EBIC and CL lay in their spatial resolution coupled with their analytical capability. The analysis of individual dislocations was necessary to determine the relative recombination strengths of edge and screw, unit and dissociated, and in semiconducting compounds of α and β type dislocations, and to make it possible to separate the intrinsic and extrinsic (impurity related) dislocation effects from those of deformation debris.

The Charge-Controlled Recombination Theory of EBIC Contrast

Important work was done by Ourmazd *et al.* (1983) and Wilshaw *et al.* (1983) originally on dislocations in transistors and later on specially deformed crystals. This identified major sources of experimental difficulty and produced information on the temperature and injection level dependence of the EBIC contrast of some dislocations that proved important for understanding their properties. This led Wilshaw and co-workers to develop a quantitative theory of the SEM EBIC contrast of dislocations (Wilshaw and Booker, 1985; Wilshaw and Fell, 1989; Wilshaw *et al.*, 1989; Fell and Wilshaw, 1991; Galloway *et al.*, 1993). This assumed, as did Morrison (1956) and Figielski (1978), that the rate of recombination via dislocations is charge controlled and identified the processes involved in recombination especially the rate limiting step. This CCR (charge-controlled recombination) theory will be briefly outlined below. Recently, Raza and Holt (1995) also applied Wilshaw's ideas to discuss the temperature dependence of the EBIC contrast of grain boundaries in polycrystalline silicon solar cells.

The Wilshaw model of charge controlled equilibrium rate recombination at dislocations treats the equal rates of capture of electrons and holes as follows. For the net rate of capture of electrons per unit length of dislocation they write (see Fig. 6):

$$J_e = J_i - R = \{C_e N_d[(1 - f)n_o \exp(-q\phi/kT) - fN_c \exp(-q\phi_o/kT)]\} \quad (3)$$

where C_e is the probability of an individual electron making the transition to or from a dislocation state, N_d is the number of states per unit length of the dislocation, f is the fraction of these states that are occupied, N_C is the density of states in the conduction band and ϕ and ϕ_o

are the potential barriers against free electrons jumping into and being re-emitted from the dislocation states, respectively.

Since, following Donolato (1978/1979, 1985), the dislocation acts as a cylinder of radius r_d in which the minority carrier lifetime is reduced from the bulk value τ to τ', the rate of hole capture per unit length is

$$J_h = (\pi r_d^2 \Delta p) / \tau' \quad (4)$$

where Δp is the hole density. Hence from eq. (2), the dislocation strength is:

$$\gamma = [(\pi r_d^2) / (D_h \tau')] = [J_h / (\Delta p D_h)] \quad (5)$$

In equilibrium we must have,

$$J_h = \gamma \Delta p D_h = J_e = J \quad (6)$$

where J is the dislocation recombination current. Hence, from eq. (3):

$$\Delta p D_h \gamma = C_e N_d [(1 - f) n_o \exp(-q\phi/kT) - f N_c \exp(-q\phi_o/kT)] \quad (7)$$

so:

$$-(q\varphi / kT) = \ln\{[\Delta p D_h \gamma + C_e N_d f N_c \exp(-q\phi_o/kT)] / [C_e N_d (1 - f) n_o]\} \quad (8)$$

Substituting from eq. (6) and making use of the fact that $-\ln(x) = \ln(1/x)$:

$$\phi = (kT/q) \ln\{[C_e N_d (1 - f) n_o] / [J + R]\} \quad (9)$$

where $R = [C_e N_d f N_c \exp(-q\phi_o/kT)]$ is the rate of re-emission of electrons from unit length of dislocation (see eq. (3)).

Substituting from eq. (1) for πr_d^2 in eq. (2):

$$\gamma = [Q / (n_o q D_h \tau')] \quad (10)$$

Assuming, for simplicity, at the moment, that $\phi = \alpha Q$ and then, substituting for ϕ from eq. (9):

$$\gamma = [kT/(\alpha q^2 n_o D_h \tau')] \ln\{[C_e N_d (1 - f) n_o]/[J + R]\} \quad (11)$$

Wilshaw *et al.* (1989) give reasons for believing D_h is nearly independent of temperature and Donolato had shown that the dislocation contrast is proportional to the defect recombination strength, so:

$$C = \{(\beta T)/(n_o)\} \ln\{[C_e N_d (1 - f) n_o] / [J + R]\} \quad (12)$$

where β is a constant depending on the microscope operating parameters and the specimen geometry (dislocation depth etc).

On the charge controlled recombination theory, eq. (12) governs EBIC contrast. This depends on the relative magnitudes of J and R. The recombination rate J will be $>>$ R if large beam currents are used (and hence, large excess minority carrier densities Δp are generated) so the flow of electrons and holes into the dislocation, J, is large or if the rate of escape of electrons from the dislocation, R, is small (because there is a small number of states in the gap, N_d, and hence few trapped electrons that could be re-emitted or because the levels are deep within the gap so the height of the barrier against electron emission, ϕ_o, is large). In such cases, eq. (12) reduces to:

$$C = [(\beta T)/(n)] \ln\{[C_e N_d (1-f) n_o]/[\Delta p \gamma D_h]\} \quad (13)$$

and the charge on the dislocation is increased above its equilibrium value (since J, the capture rate, $>>$ R, the re-emission rate). For a constant beam current, C is approximately proportional to T (regime 1 in Fig. 7d) while at constant temperature, C is approximately proportional to $-\ln(I_b)$ (since Δp is proportional to I_b) as shown in Figure 8.

To discuss the implications of the theory, Wilshaw (1989) also obtained numerical solutions for γ and hence the contrast C from eq. (12) for suitable values of the parameters. This was done using, instead of the simplifying assumption, $\phi = \alpha Q$, employed above, the more accurate expression obtained by Masut *et al.* (1982):

$$\phi = \{(Q)/(2\pi\epsilon\epsilon_o)\} \{\ln[(\lambda_D Q)/(q)] - 0.5\} \quad (14)$$

where ϵ and ϵ_o are the relative and free space permittivities, respectively, λ_D is the Debye length and q is the charge on the electron. Proceeding in this way, it was shown that two forms of variation of contrast C with temperature could be obtained as shown in Figure 7d depending on the relative density of trap centers along the dislocation line, N_d.

The physical mechanisms underlying the curves in Figure 7d can be explained by reference to the three possibilities shown in Figures 7a, 7b and 7c. If the trap states were to lie above the Fermi level (Fig. 7a), the dislocation would be uncharged and the theory would not apply. The only possibilities then are for the dislocation states to fall below or on the Fermi energy level.

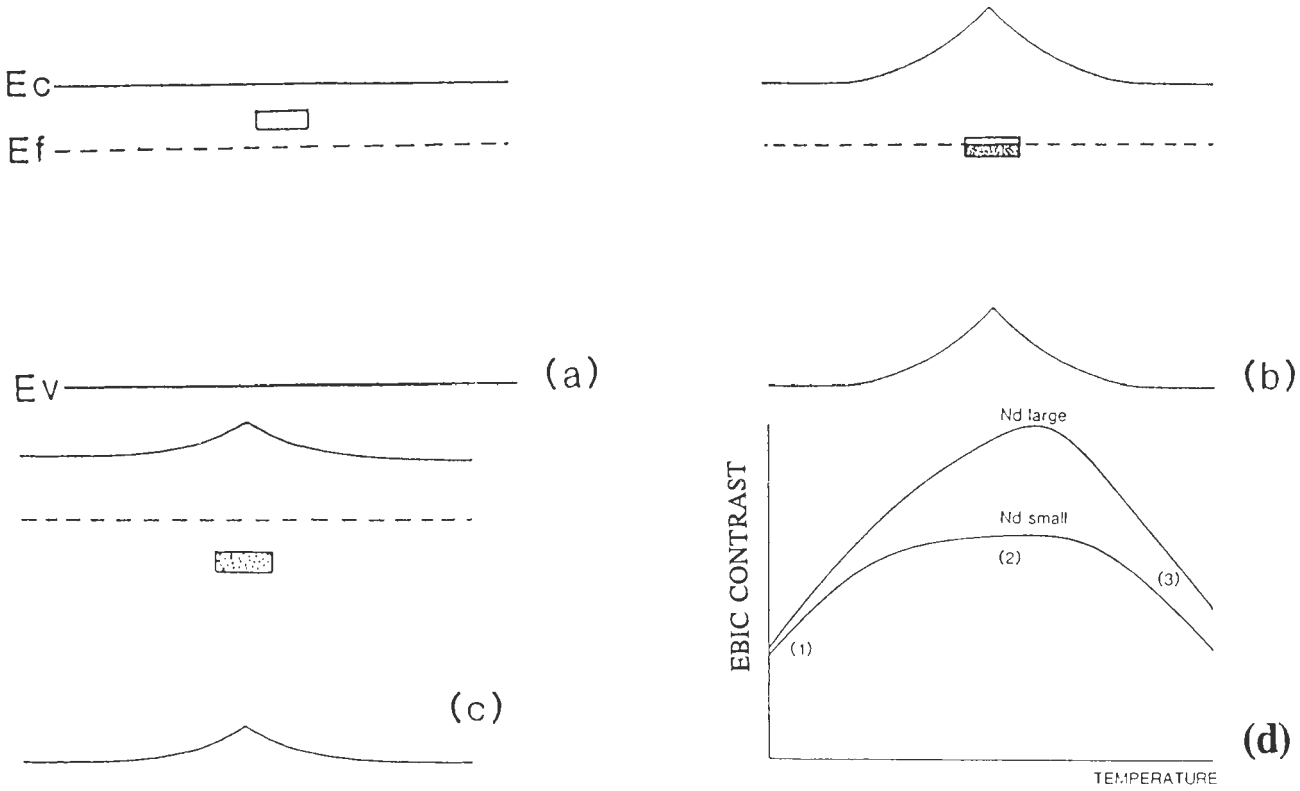

Figure 7. Relative to the Fermi level, the narrow dislocation recombination band of trap states, represented by the box in the gap, can either (a) lie above it, (b) be pinned to it or (c) fall below it. (d) The three regimes of temperature dependence of EBIC contrast predicted by the Wilshaw theory. Situation (b) (band pinning) leads to regime 3 while (c) leads to regime 2. (After Wilshaw and Fell, 1991 and Fell and Wilshaw, 1991).

Consider first the case that the trap states are relatively few so they can all be filled without the band bending bringing the traps up to the Fermi level (Fig. 7c). Then, a rise of temperature, producing movement of the Fermi energy down toward the intrinsic (mid-gap) position, will have no effect. In this temperature range, C is T-independent. This is regime 2 in Figure 7d. Suppose now, N_d is large, so that, with the traps partially filled, their energy rises to the Fermi level (Fig. 7b). The trap level becomes "pinned" to the Fermi level and as the latter moves down with increasing T, the traps must empty. This means that the charge Q and hence the dislocation recombination strength γ and the EBIC contrast C will fall with T. As the temperature continues rising and the Fermi level falling, this situation is eventually reached, even for small N_d. This is regime 3 in Figure 7d.

These predictions were found to be in agreement with experimental results. The predicted $C \propto \ln(I_b)$ behaviour mentioned above was confirmed by measurements on relatively clean dislocations (produced by high-low T deformation but not in transition-metal-free material) in Si at low temperatures and high beam currents (Fig. 8) by Wilshaw and Fell (1989).

At relatively high temperatures and small beam currents R > J and eq. (12) takes the form:

$$C = [(\beta T)/(n_o)] \ln\{[C_e N_d(1 - f)n_o]/ [(C_e N_d f N_c)\exp(-q\Phi_o)/(kT)]\} \quad (15)$$

so the contrast is independent of the beam current as confirmed by the low current region of Figure 8.

Fundamental Dislocation Parameters Obtained from EBIC Contrast on the CCR Theory

If the experimental conditions are selected so the contrast falls into one of the three temperature dependence regimes of Figure 7d or measurements are made at constant T as a function of I_b as shown in Figure 8, data can be obtained that can be quantitatively compared with theory. Fitting such data to simulated curves obtained by numerical solution of eq. (12), modified in accordance with eq. (14), can be used to determine

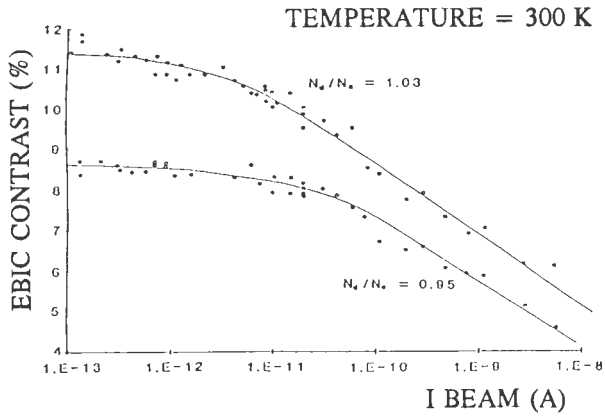

Figure 8. The variation of EBIC contrast with $\ln(I_b)$ for two screw dislocations in n-type 10^{15} cm^{-3} silicon (experimental points) and curves calculated from the Wilshaw theory. (After Wilshaw *et al.*, 1989).

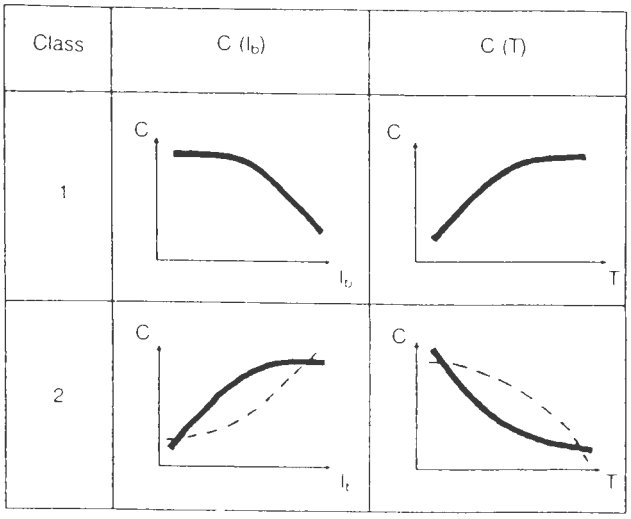

Figure 9. Schematic diagrams of the two experimentally observed forms of variation of EBIC contrast C with beam current and with temperature. The two types of behaviour are tabulated as those of Classes 1 and 2. (After Kittler and Seifert 1993b).

---

values for some fundamental parameters of the dislocation under examination. In general, not all the parameters can be obtained at once. For detailed discussions, see papers from Wilshaw's group (mentioned above). For brevity, only the main conclusions from that work are summarized here.

Wilshaw and Booker (1985) and Wilshaw *et al.* (1989) made measurements on high purity, float-zone-grown n-type (10^{15} cm^{-3}) Si deformed under clean conditions in two stage compression at 850°C (to generate dislocations initially) and 420°C to multiply and move dislocations with minimal point defect diffusion. This procedure, developed by Wessel and Alexander (1977), produces relatively clean dislocation cores (but transition metal contamination can only be avoided by using transition-metal-free material and non-metallic deformation apparatus, as we will see below). The specimens contained large dislocation loops. The result of fitting the data that Wilshaw and Booker (1985) obtained to the calculated CCR curves was that N_d (the number of dislocation states per unit length) $\approx 2 \times 10^6$ cm^{-1} for the screw and about 10% higher for the 60° dislocations investigated with an accuracy not better than 20 or 30%. These relatively low line densities of dislocation states are in agreement with the DLTS results of various groups on bulk deformed material. Wilshaw and Booker (1987) found that the EBIC contrast was not strongly dependent on ϕ_o (the energy depth of the states below the conduction band edge) which could not therefore be evaluated. However, from their data, the charge on the dislocation per unit length was $Q = 2.6 \times 10^{-13}$ C cm^{-1}. Hence, the band bending could be calculated. Since the theory was applicable, the dislocations apparently had a negative charge, so the defect states must lie below the Fermi level, which can be calculated for 10^{15} cm^{-3} material at 350°C. This lead to the conclusion that the defect level for both screw and 60° dislocations is at approximately mid-gap depth.

Wilshaw and Fell (1989, 1991) compared dislocations introduced as before by deformation at 420°C which gave EBIC contrast of $\approx$ 13% and others introduced by 650°C deformation which gave only $\approx$ 2%. The 650°C deformation dislocations were found to have a line concentration of states $N_d \approx 5 \times 10^5$ cm^{-1} (compared to 2×10^6 cm^{-1} for the 420°C ones) and these states could only be determined to lie deeper in the gap than 0.3 eV (0.34-0.37 eV below E_c according to Fell and Wilshaw, 1991). These results were in good agreement with the results of DLTS and EPR measurements on similar specimens (Omling *et al.*, 1985; Weber and Alexander, 1983) provided the correct DLTS signals are considered (for details, see, Wilshaw and Fell, 1989). Measurements on the curved dislocation segments at the corners of the loops gave the same value of N_d as the straight segments along the sides of the loops. Since there must be high concentrations of kinks to take the curved segments out of alignment with the Peierls troughs, this shows that the kinks do not introduce deep trap sites. Hence, they are apparently not the "special sites" thought to be responsible for the few dangling bond type centers.

Wilshaw and Fell (1991) and Wilshaw *et al.* (1991) also began a study of the effects of impurity contamina-

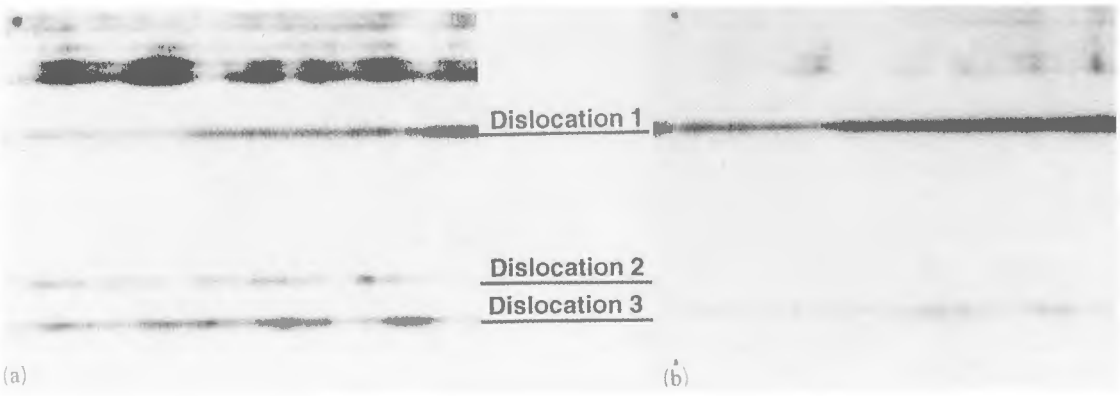

Figure 10. EBIC micrographs of misfit dislocations at the interface of a p-type, Cu-contaminated $Si_{0.98}Ge_{0.02}$/ Si sample at (a) 80K and (b) 300K. Dislocation 1 is of class 1 and dislocation 2 of class 2. Dislocation 3 exhibits intermediate ("mixed") behaviour. (After Kittler *et al.*, 1994).

tion. They found that deliberate copper contamination of 650°C deformation dislocations resulted in ≈ 7% contrast which is much higher than for the uncontaminated ones (2%) but less than for the 420°C dislocations (13%). The work referred to showed that dislocations could be produced with sufficiently low line densities of states so they can fill without pinning the Fermi level so it can lie well above the dislocation energy level (Fig. 7c). Such dislocations will exhibit the regime 2 (T-independent C) behaviour of Figure 7d. Addition of further states by copper contamination could be sufficient to alter the situation to that of Figure 7b. They also studied oxidation induced stacking faults (OISFs) in silicon. When uncontaminated, these gave no EBIC contrast. Iron contamination gave strong contrast at the bounding partial only, while copper contamination also gave weaker contrast from the fault. The iron contaminated OISFs gave ≈ 18% contrast for the partial dislocations. The Cu-contaminated OISFs gave 30 to 40% contrast using a 15 kV beam. This is so large that, it was suggested, it could not all be due to recombination but that a significant contribution was due to a reduction in the electron-hole pair generation rate. In both cases, contamination was sufficiently heavy to lead to precipitation and the different effect of the two impurities was ascribed to differences in their precipitation.

Fell and Wilshaw (1991) reported that the results obtained by Wilshaw in his PhD work on samples deformed at 420°C in Cologne by Alexander's group and on specimens similarly deformed in Oxford years later gave "identical" results, showing that good sample-independent reproducibility had been attained. They also extended the analysis of the contamination results reported above. They concluded that copper contamination did not alter the values of N_d or E_d (the dislocation trap energy level) for the 420°C dislocations. The 650°C copper decorated dislocations, however, showed much higher (≈ 8%) contrast with an occupation limit 0.48 to 0.51 eV below Ec (the conduction band edge). They concluded that the high stress needed to deform Si at 420°C produces a deep level (> 0.53 eV) which they thought to be intrinsic to the dislocation core structure. Copper decoration introduces a relatively deep level (0.48 to 0.51 eV), but as these states lie above the Fermi level, they do not affect the dislocation recombination strength. A shallower (0.34 to 0.37 eV) defect level of unknown origin is present in 650°C deformed dislocations which may be due to residual impurities and is lifted above the Fermi level when copper is added. A further critical account of this work was given by Wilshaw *et al.* (1991).

Other Forms of Dislocation Contrast Variation with Temperature and Beam Current

Wilshaw *et al.* (1989) made measurements on dislocation loops introduced by microhardness indentor in 5 x 10^{15} cm^{-3}, n-type GaAs. They found that the contrast increased with increasing temperature. The EBIC contrast fell with increasing I_b, but unlike silicon dislocations in regime 1 of Figure 7d, it was not proportional to $\ln(I_b)$ as in Figure 8. The variation continued to the lowest attainable beam currents possibly indicating that the dislocation charge is far from equilibrium unlike 60° and screw dislocations in Si.

Studies of α, β and screw dislocations created by microindentation and subsequent bending of GaAs specimens of liquid encapsulated Czochralski (LEC), liquid

phase epitaxy (LPE) and metal-organic chemical vapor deposition (MOCVD) material were reported by Galloway *et al.* (1993). All the dislocations in LEC and LPE material behaved similarly and their recombination strength increased with decreasing temperature. The results on the purer MOCVD GaAs were different and Galloway *et al.* (1993) concluded that different recombination centers were active in this material. Large differences were found depending on the way the dislocations were produced, suggesting either a dependence on the different core structures or point defect decoration of the dislocations.

The Shockley-Read-Hall recombination model for dislocation EBIC contrast

Kittler and Seifert (1993a,b) pointed out that the literature on silicon contained reports of the observation of the two (class 1 and 2) distinct forms of variation of dislocation dark EBIC contrast with T and I_b (Fig. 9). Class 1 is the form of behaviour analysed by Wilshaw and coworkers, i.e., charge controlled recombination (CCR) like behaviour as reported and referenced above.

Kittler *et al.* (1994) showed a particularly impressive example of opposite signs of variation of EBIC contrast, C, with temperature among parallel misfit dislocations in Cu-contaminated p-type SiGe on Si as shown in Figure 10. Clearly, dislocation 1 has increased C as T increased while dislocation 3 has decreased in contrast and dislocation 2 has fallen to invisibility. The measured values of C versus T for these dislocations are shown in Figure 11a.

Kittler and Seifert (1994) proposed an alternative treatment for both the forms of behaviour of Figure 9. This is based on Donolato's expression (for an account of this work with full references see, e.g., Holt, 1989) for the EBIC contrast of a dislocation:

$$C \propto \{1/(D\tau')\} \tag{16}$$

They assumed that recombination in the defect region is due to a single type of recombination centre obeying Shockley-Read-Hall (SRH) theory, i.e., that recombination takes place via independent centers, not at interacting charge-controlled centers as in the Wilshaw theory. The SRH recombination theory (see, e.g., Sze, 1985, pp. 44 *et. seq.*) gives the net rate of carrier recombination U as:

$$U = \{(np - n_i^2) / [(n + n_1)\tau_{po} + (p + p_1)\tau_{no}]\} \tag{17}$$

where

$$\tau_{po} = \{1/[(N_t\sigma_p) < \nu th >_p]\} \tag{18}$$

$$\tau_{no} = \{1/[(N_t\sigma_n) < \nu_{th} >_n]\} \tag{19}$$

$$n_1 = N_C \exp[(E_tE_c)/(kT)] \tag{20}$$

$$p_1 = N_V \exp[(E_v - E_t)/(kT)] \tag{21}$$

Here, n and p are non-equilibrium electron and hole concentrations, n_i is the intrinsic carrier concentration; τ_{no} and τ_{po} the minority-carrier lifetimes, σ_n and σ_p capture cross sections, and $< \nu_{th} >_n$ and $< \nu_{th} >_p$ are the average thermal velocities for electrons and for holes, respectively. N_t is the trap concentration, E_t is the trap level, E_V and N_V are the (maximum) energy and the density of states in the valence band; the other quantities have their usual meanings.

Since

$$n = n_o + \Delta n \text{ and } p = p_o + \Delta n \tag{22}$$

where n_o and p_o are the equilibrium electron and hole densities and Δn is the concentration of injected carriers, and since, by definition,

$$\tau' \equiv (\Delta n)/(U) \tag{23}$$

we obtain:

$$\tau' = \{[(n_o + n_1 + \Delta n)\tau_{po} + (p_o + p_1 + \Delta n)\tau_{no}] / [n_o + p_o + \Delta n]\} \tag{24}$$

Assuming, for the p-type material of Figure 10, that $\tau_{po} = \tau_{no} = \tau_o$ and that n_o is negligible, eq. (24) can be simplified to:

$$\tau' = \tau_o [1 + 2\beta + (n_1)/(p_o) + (p_1)/(p_o)]/(1 + \beta) \tag{25}$$

where $\beta = \Delta n/p_o$ is the injection level.

Eq. (25) substituted into eq. (16) was used to simulate the form of dependence of dislocation contrast on T and on the injection level, i.e., on I_b. For this purpose, Kittler and Seifert (1994) assumed that D was independent of T which, since $D \propto \mu T$, implies that $\mu \propto T^{-1}$. They found that the form of variation of C with T on this model depends essentially on the depth of the independent recombination centers as shown in Figure 11b. That is, deep centers, as in the 0.55 eV (mid-gap) case, lead to $C \propto T^{1/2}$ due to the T dependence of the thermal velocity. The form of dependence of the shallow centers, as in the case for those at a depth of 0.075 eV in Figure 11b, is due to changes in the occupation of the centers consequent on the movement

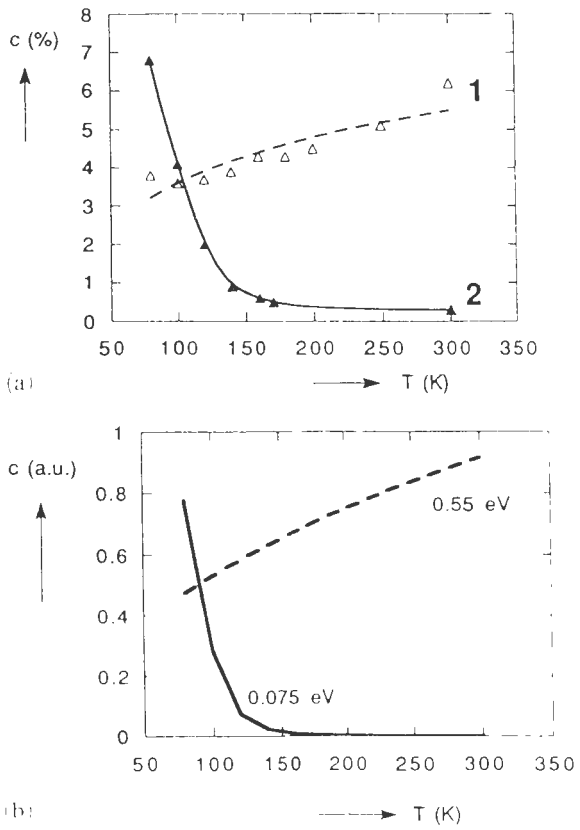

Figure 11. Variation of EBIC contrast with temperature: (a) experimental data for dislocations 1 and 2 and (b) simulated behaviour for dislocations with independent (Shockley-Read-Hall) recombination centers with energy levels at depths of 0.075 and 0.55 eV. (After Kittler and Seifert 1994.)

---

in the Fermi level, which does not affect the occupation of the deep centers.

The measured variation of C with I_b, i.e., with injection level, β, for the two dislocations is shown in Figures 12a and 12c. The simulations of this dependence for independent centers with the same shallow and deep levels as before are shown in Figures 12b and 12d. The form of variation of C with I_b (β) is the same for both shallow and deep centers at low temperatures but at room temperature the shallow centre case shows a slight increase of C with I_b (β).

The agreement in form between experimental and simulated curves in Figures 11 and 12 is striking and the ability to account for both forms of behaviour with a single model is attractive. Testing the model on a wide range of dislocations produced in a variety of ways, in the manner of Wilshaw's group, remains to be done, however. This should include careful fitting of experimental data to simulated curves to obtain quantitative values for recombination levels, etc.

Discussion: The Two Types of Dislocation Recombination Theory

It is now clear that there are opposite types of temperature dependence possible even for neighbouring dislocations (Fig. 10). The dislocation EBIC behaviour of class 1 in Figure 9 can apparently be accounted for by either of two theories: those of the "charge-controlled" or the "deep-independent-centre" models of recombination. Class 2 behaviour can apparently be accounted for by the "shallow-independent-centre" model.

Are both types of model physically reasonable? The SRH theory is known to work well for independent, impurity atom recombination centers. The only question then is: do the dislocation recombination centers act independently? Consider now the charged dislocation recombination model. Read (1954b) developed several treatments of the occupation fraction for an assumed density of one trap state per atomic distance along the dislocations. These assumed that the dislocation traps filled due to electrons dropping from the conduction band into the traps to lower their energy until the rising electrostatic energy due to the repulsion of the charged line for further electrons made it energetically unfavorable for any more to be trapped. This approach led to the conclusion that about one in ten traps would be filled at room temperature. It is now known that trap states only occur at intervals of about one hundred atomic spacings along partial dislocations, so trap states occur about every fifty atomic distances along extended unit dislocations. Consequently, the rising electrostatic energy of the trapped charges is a less severe limitation than Read (1954b) expected and complete trap filling is possible. Thus, provided the density N_d is small in Figure 7d, as the Fermi level rises through the trap energy level as the temperature is lowered, the traps can go from empty to full, i.e., the trap states all capture electrons on the CCR model. For lightly doped (10^{15} cm^{-3}) material, the space charge cylinder radius is then about 0.15 μm (Wilshaw, private communication) rather than the 1 μm given by the model of the dislocation used by Read with its hundred times higher trap density. This radius is still much larger than the fifty or one hundred interatomic distances between charged traps, i.e., say 100 $a_o/\sqrt{2}$ (where a_o is the lattice constant of silicon) = 38.4 nm. Thus, the continuum-like charged line and surrounding compensating space charge cylinder picture is self consistent, involving reasonable magnitudes for the parameters of the model.

Are there reasons to think that the traps would not

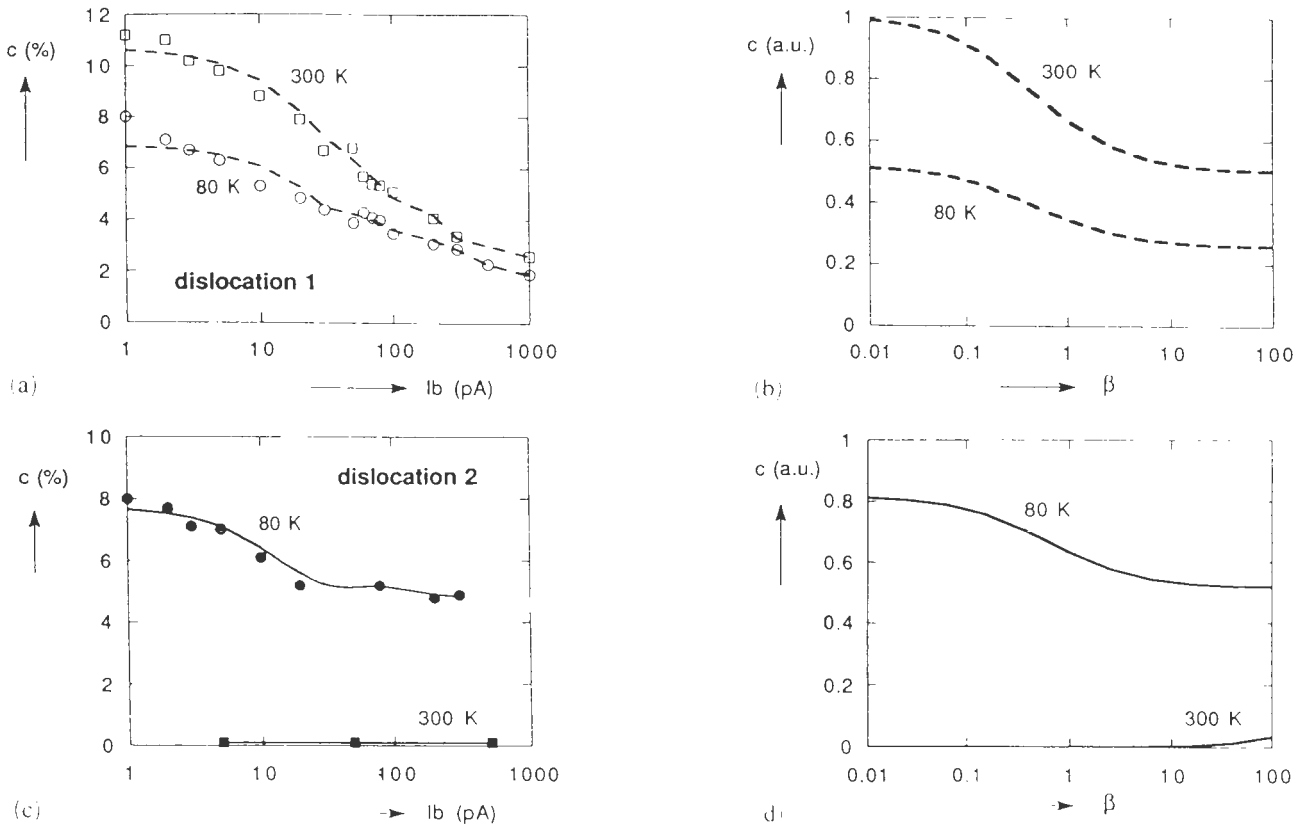

Figure 12. Experimental data for the variation of EBIC contrast with I_b is shown in (**a**) for dislocation 1 and in (**c**) for dislocation 2. Simulated curves of the variation of C with injection level β at the two temperatures marked are shown for dislocations with independent recombination centers with energy level depths in (**b**) of 0.55 eV and in (**d**) of 0.075 eV. (After Kittler and Seifert 1994).

act as independent centers but give rise to an effective line charge? At these spacings, it seems likely that the wave functions of the trap states begin to overlap so the energy levels broaden into a narrow band as Shockley (1961) and Labusch and Schroter (1978) assumed. Experimental evidence of the conduction along dislocation lines due to this delocalization was found at low temperatures and microwave frequencies by Ossipiyan (1981, 1983). In addition, the idea of charge-controlled recombination is supported by the earlier success of charged dislocation models that were used to account for electrical noise (Morrison, 1956) and the influence of dislocations on conductivity (Labusch and Schroter, 1978) and on photoconductivity (Figielski, 1978).

The CCR theory is also supported by a substantial body of experimental work on dislocations exhibiting the CCR (class 1) form of EBIC contrast behaviour. It was seen above that these data could be accounted for by the theory and that curve fitting lead to values for dislocation parameters (e.g., N_d) that are in good agreement with values obtained by independent methods (ESR in the case of N_d).

The Shockley-Read-Hall model for dislocation EBIC contrast has been worked out in less detail but appears to require implausible magnitudes for some parameters. Thus, in an early paper, Kittler and Seifert (1981) proposed on SRH theory that:

$$\gamma = N_d \, \sigma \, v_{th}$$

where σ is the capture cross section of the independent traps (assumed to be atom-sized so $\sigma = 10^{-14}$ cm^{-2}) and v_{th} is the thermal velocity of the minority carriers. They used this expression to determine the line density of dislocation traps, N_d, necessary to account for dislocation recombination strengths γ. They obtained, for the density necessary to account for even the minimum EBIC contrast observable (which they took to be C = 0.5%), a minimum value of $N_d = 170\ \mu^{-1}$. This should be compared with the order of magnitude spacing of traps found in recent ESR studies (and in Wilshaw's

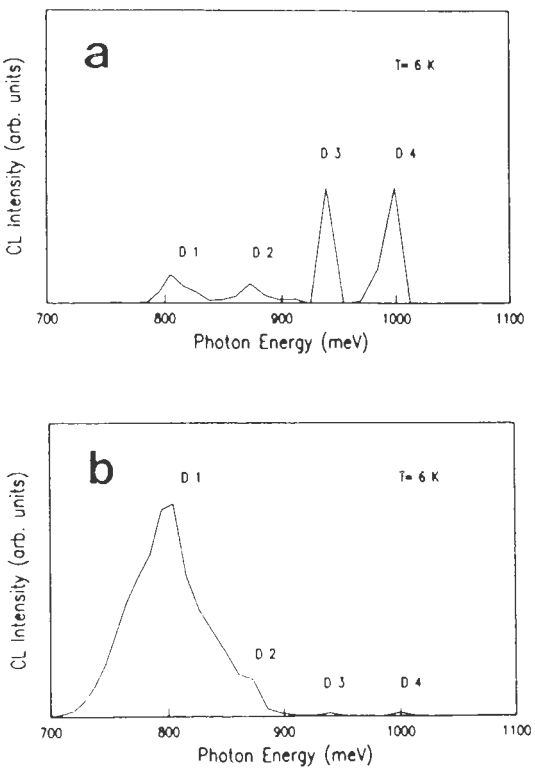

Figure 13. CL spectra of FZ Si plastically deformed at 800°C and lightly Cu contaminated (**a**) on a slip plane and (**b**) between the slip planes (after Higgs *et al.*, 1992).

EBIC contrast studies, interpreted on the charge-controlled recombination (CCR) model), 38 nm, which corresponds to a density $N_d = 1/0.038 = 26\ \mu m^{-1}$. Thus, to explain dislocation EBIC contrast, which is often an order of magnitude greater than the value used above, on the SRH model, even assuming a capture cross section that may be an order of magnitude or a bit more larger than that assumed above, still requires large trap densities compared to those found by ESR. It is also likely that at such high trap densities, wave functions overlap and consequent broadening of the trap level into a band would occur so the traps would not be independent.

It is also possible to estimate the amount of band bending, i.e., the height of the potential barrier ϕ (Fig. 4b) likely to be produced by the charged traps associated with dislocation lines. Even if the traps are shallow so E_d is small, since N_d is necessarily large on the SRH model, as the temperature is lowered, the number of trapped electron charges per unit length will become significant, so the band bending will continue until E_F becomes pinned to E_d. Since the movement of E_F from room to liquid nitrogen temperatures is much larger than kT, so will ϕ be. Thus, the height of the potential barrier will be sufficiently large to require a thermal activation term in the rate of capture for the majority carriers as is assumed by the CCR theory (eq. (7)).

What difference determines whether a dislocation has class 2 or 1 EBIC contrast properties is unclear. Wilshaw and co-workers believed their dislocations, produced by the Wessel and Alexander (1977) two-temperature deformation method, were clean. The work of Higgs and coworkers, to be discussed below, cast doubt on this belief. In addition, similarly produced 60° and screw dislocations were found to have different forms of temperature dependence of EBIC contrast (Kusanagi *et al.*, 1992) as were the apparently similar dislocations 1, 2 and 3 in Figure 10.

Thus, there are unquestionably dislocations whose EBIC contrast exhibits behaviour of class 2, not the class 1 (CCR-like) behaviour of Figures 7 and 8. This requires explanation, and perhaps SRH recombination is relevant. However, the theory needs to be developed in greater detail and checked against extensive experimental results for self-consistency and plausibility of the values of the parameters yielded by the model.

For an additional review of this field see Alexander (1994). It is hoped that the results of further experimental work, including that on III-V materials, and its analysis, should resolve the matter.

The Role of Impurities

It was quickly realized that the interaction of dislocations and grain boundaries with impurities, leading to the formation of Cottrell atmospheres and the decoration of defect cores with impurity atoms would greatly alter their electrical and optical properties. The theory and the results of extensive early studies of the effects of the segregation of donors and acceptors, oxygen, carbon and a number of metals in Ge and Si were reviewed by Bullough and Newman (1963).

D line photoluminescence and the nearly universal role of traces of transition metals

The dominant role of traces of transition metals was revealed by important recent work using a combination of SEM EBIC and CL with other powerful methods of analysis (Higgs *et al.*, 1989, 1990a,b, 1991, 1992; Higgs and Lightowlers 1992; Higgs and Kittler, 1993).

Dislocation related lines in PL spectra were identified in silicon (Sauer *et al.*, 1985). There are four lines and D1 and D2 behave similarly as do D3 and D4. D3 and D4 were ascribed to transitions in the dislocation core whereas D1 and D2 might be associated with point defects in the strain fields of the dislocations (Sauer *et al.*, 1985). Higgs *et al.* (1989) were therefore puzzled

Table 1. Results of EBIC measurements on clean and copper decorated dislocations by Fell *et al.* (1993).

Deformation temperature C	Condition	φ_o (eV) (Fig. 4b)	Relation to E_F at 350 K (Fig. 7)	N_d (10^6 cm^{-1})	EBIC contrast
900	Clean	0.31 to 0.39	pinned	> 2.12	1.5
650	Clean	0.34 to 0.37	pinned	> 1.94	1.5
650	Copper	0.48 to 0.51	pinned	> 2.83	5.0
420	Clean	> 0.52	below	2.8	6.0
420	Copper	> 0.53	below	2.88	6.0

by the absence of D line luminescence in molecular beam epitaxy (MBE) grown Si epilayers which were known by etching to contain 10^3 to 10^5 dislocations cm^{-2}. They found that D-band luminescence could be produced by deliberate contamination with transition metals.

Higgs *et al.* (1990a) then examined several ingots of floating zone (FZ) Si using a heat treatment and PL spectral test known to detect transition metals and sensitive to copper surface concentrations as low as 10^{10} cm^{-2} (Canham *et al.*, 1989). They found one FZ ingot that showed no traces of transition metals and from this cut specimens that were strained using the high-low temperature deformation technique of Wessel and Alexander (1977), in special quartz rigs to avoid metallic contamination. In such material, dislocations produced in this way with cores free of transition metal contamination, produced very little electron-hole recombination, i.e., no D lines in the PL spectrum nor any dark line EBIC contrast (Higgs *et al.*, 1990a,b). All these effects immediately appeared strongly, however, if the silicon was lightly brushed with a Cu wire and heated. Transmission electron microscopy (TEM) examination showed no impurity precipitation on the dislocations.

Higgs *et al.* (1991) extended this work to include both dislocations in deformed FZ Si and oxidation-induced stacking faults in chemical vapor deposited (CVD) Si. EBIC dark contrast was observed at the defects whether they were transition metal contaminated on an atomic scale or by precipitates. However, the D line PL was lost as the contamination was increased to the level at which precipitation occurred. For both light and heavy contamination, the EBIC contrast followed the injection level dependence predicted by the theory of Wilshaw. Higgs and Lightowlers, 1992 and Higgs *et al.* (1992) reported that D line PL and EBIC contrast could be detected when clean dislocations were lightly contaminated with Cu, Fe, Ni, Ag or Au.

Higgs and Lightowlers (1992) and Higgs *et al.* (1992) also exploited the spatial resolution of CL to show that the D3 and D4 emission was associated with the dislocation lines whereas the D1 and D2 line emission came from between the dislocations (due presumably to transition metal contaminated debris) as shown both by spectroscopy (Fig. 13) and CL monochromatic imaging (Fig. 14).

It was reported that dislocations in $Si_{1-x}Ge_x$/Si also were inactive as regards D-line PL, EBIC and CL until lightly contaminated with a transition metal (Higgs and Lightowlers, 1992; Higgs and Kittler, 1993).

Fell and Wilshaw (1991), and Wilshaw and Fell (1991) applied the Wilshaw theory to the EBIC contrast of clean dislocations produced by low (420°C) and higher temperature (650°C) strain in Si and the effects of Cu and Fe contamination as reviewed above. Fell *et al.* (1993) also studied the effects of both copper and nickel contamination of dislocations in silicon and reported the data listed in Table 1. They found an "electron beam induced activity" effect, i.e., changes in EBIC contrast produced by electron bombardment.

Passivation

While donor and acceptor impurities and transition metals produce electrical effects, other elements do not. Some even suppress or neutralize the electrical and optical activity of defects. Most important of these are hydrogen and chlorine. Hydrogen is well-known for its use to passivate dangling bonds in non-crystalline ("amorphous") Si and to neutralize grain boundaries in polycrystalline Si solar cells (Raza and Holt, 1991). Higgs and Kittler (1995) carried out an EBIC contrast analysis of the effects of hydrogen plasma treatment on misfit dislocations in SiGe/Si epilayers. They reported that 90% of the shallow states associated with the dislocations were unaffected, whereas the deeper mid-gap states were readily passivated. They also studied the effects of oxygen on dislocations in Czochralski silicon. The samples contained oxygen concentrations from 10^{17} to 10^{19} cm^{-3}. These samples were scratched to nucleate dislocations and deformed in bending. Dislocations, produced by plastic deformation at 700°C for 15 minutes, emitted dislocation D-line PL, but after longer

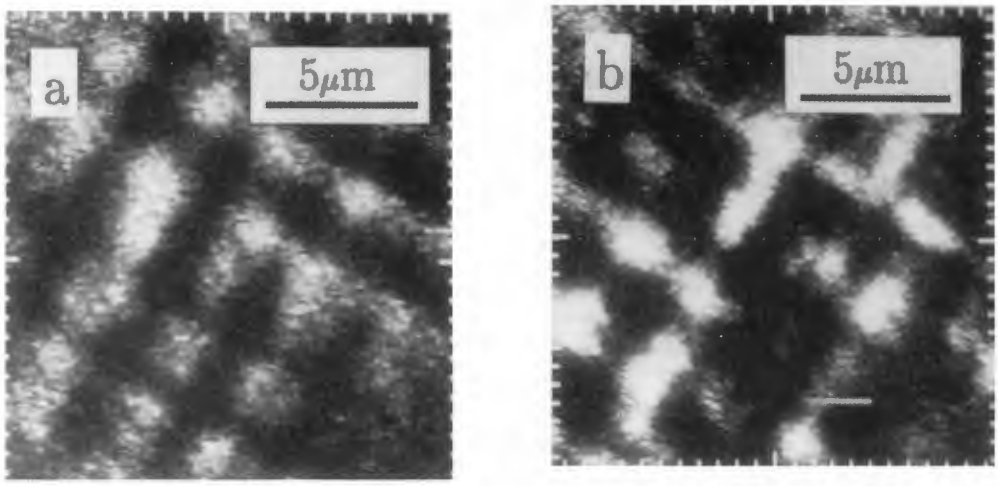

Figure 14. Monochromatic CL images from a Ni contaminated SiGe/Si epilayer taken through (a) a D2-transmitting filter and (b) a D4 filter (after Higgs and Lightowlers, 1992).

deformation times, the PL was quenched. EBIC measurements showed that the dislocations exhibited deep level recombination. They suggested that the interaction of dislocations with oxygen produced predominantly deep level states that quench the radiative recombination (Higgs and Kittler, 1995).

The Electronic Energy Levels and Bands of Dislocations

Castaldini *et al.* (1987), Castaldini and Cavallini (1989), and Cavallini and Castaldini (1991) introduced the technique of QIRBIC (quenched infrared beam induced current). In this mode, dislocations are observed by LBIC (light or laser beam induced current; or it can be by EBIC) by scanning the top surface while from below the Si sample is irradiated with infrared light of variable, less than band gap photon energy (Fig. 15). As the wavelength is varied, absorption will occur whenever the photon energy becomes equal to one of the activation energies for transitions between a dislocation energy level and either the conduction or valence bands or between two dislocation levels.

They found direct evidence that dislocations do have complex energy level diagrams as shown in Figure 16. On the Donolato theory, contrast is proportional to dislocation strength, and according to the Wilshaw theory, the dislocation strength is proportional to the charge per unit length of dislocation line, Q. Hence, on CCR theory, Figure 16 is a plot of the variation of Q with photon energy with peaks at values of transition activation energies. The defect energy spectrum will thus be observed directly with the spatial resolution required to analyse single defects whose structure can be subsequently determined by TEM or otherwise.

Another scanning beam technique that has recently been used to study the energy levels of individual dislocations is SDLTS (scanning deep level trap spectroscopy) (Petroff and Lang, 1977; Petroff *et al.*, 1978; Breitenstein and Heydenreich, 1985; Breitenstein, 1989; Schroter *et al.*, 1989).

Conclusions Concerning the Effects of Dislocations in Semiconducting Materials

Lately, tremendous progress has been made, especially by applying powerful scanning beam techniques such as SEM EBIC and CL, and QIRBIC to determine the properties of individual defects in the most highly pure and perfect material now available. This has succeeded in clarifying a number of questions that were controversial for a long time, such as the roles of point defects produced by plastic deformation and of impurity contamination. The main conclusions that can now be drawn are as follows:

(1) There are two types of behaviour of dislocation EBIC dark contrast in Si-based materials. One form can be treated by assuming that the dislocations are charged, giving rise to band bending and that this controls recombination (the Wilshaw theory). Alternatively, the Shockley-Read-Hall (SRH) theory for isolated point recombination centers can be applied and the two forms of behavior explained as corresponding to deep and shallow centre recombination. The validity and range of applicability of these models (e.g., to dislocations in III-V materials?) remain to be determined.

(2) There are several levels, deep and shallow, associated with dislocations and some of these levels are impurity-associated or activated (e.g., those responsible for the D line PL and EBIC dark contrast) by the traces of Cu etc almost always found in samples of silicon. Some can also be passivated by hydrogen. The types of

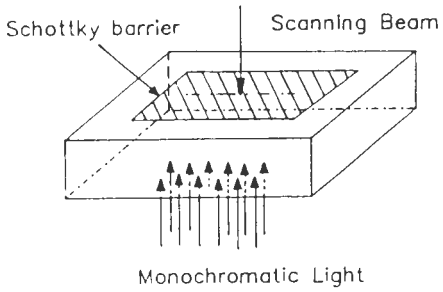

Figure 15. Diagram illustrating the principle of the QIRBIC (quenched infra-red beam induced current) method (after Castaldini and Cavallini, 1989).

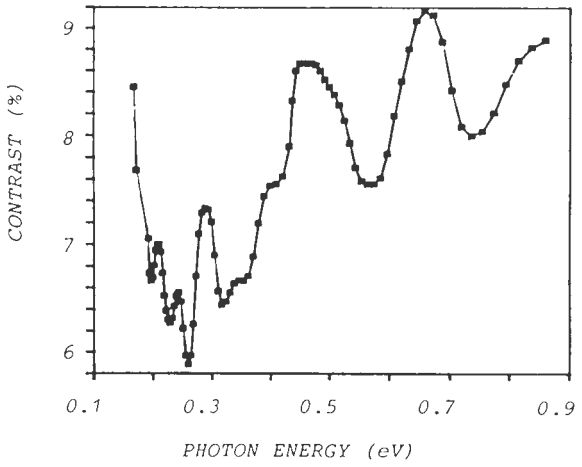

Figure 16. QIRBIC contrast versus photon energy for a dislocation in silicon (after Castaldini and Cavallini, 1989).

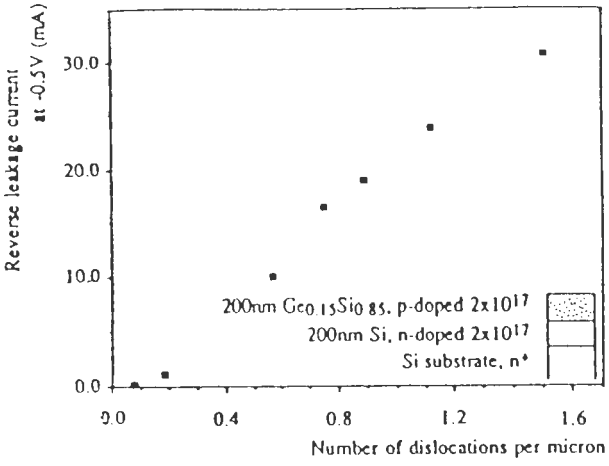

Figure 17. Reverse leakage current through a 3 mm diameter diode versus the number of dislocations cutting a line (dislocation density) (after Ross *et al.*, 1993b).

Table 2. Leakage current per stacking fault deduced from electrical measurements and stacking fault counts (see Ogden and Wilkinson (1977) for references to the sources of the data listed).

Leakage current per stacking fault	Year reported
15 - 500 μA	1973
60 nA - 6 μA	1974
7 pA - 33 pA	1976
$\approx$ 10 pA	1976
4 - 590 pA	1977

centre present vary with the type of dislocation and the type and amount of contamination. QIRBIC appears to be the best means for studying dislocation (and grain boundary) energy spectra, both intrinsic and impurity activated or passivated.

(3) There are also a majority of plastic deformation generated centers (e.g., those producing the D1 and D2 PL lines) that are not associated with the dislocation lines but with points remote from the dislocations (debris).

Thus, while progress is rapid, there are still many unsolved problems even concerning dislocations in Si-based materials. The fundamental study of defects in the III-V compounds using the powerful new methods has only begun (e.g., Galloway *et al.*, 1993), and in the II-VI compounds, it has not yet begun. There is also a need to relate the work on the effects of plastic deformation on electrical conductivity (Labusch and Schroter, 1978) and on photoconductivity (Figielski, 1978) to the information from recent advances.

The Role of Defects in Devices

Defects can have two types of effect on devices: immediate effects; and those that involve microstructure growing or changing during device operation, leading to early failure. Following the first observations of physical parameter defect density correlations in devices produced at any one time (such as in Fig. 2), it was found that there is also a year-by-year improvement of device performance and yields, the so-called "time effect". This type of improvement is not always correlated with the dislocation density. One reason that sometimes it is not is that, with time, there is a reduction in the effect per defect in a particular type of device. An example is the steady fall in the leakage current per stacking fault in Si p-n junctions and CCD devices, deduced from electrical measurements and stacking fault counts by a

number of workers as listed in Table 2 (Ogden and Wilkinson, 1977). They suggested that this was essentially due to reductions in the amount of decorating impurity with time.

A further major cause of poor correlation is that numerous defects can occur in the material outside the small active volume of the device(s) and so have no direct effect on performance. This is particularly the case in Si (and GaAs) integrated circuits in which the wafer is typically 400-500 μm thick but the planar technology devices are formed in a top layer only one or a few μm in depth (Holt, 1979). Defects in the wafer "substrate" below the active device volume can have only indirect or delayed effects. A valuable indirect effect is the impurity gettering that can result from defects deliberately introduced by damaging the back side (bottom) of Si wafers. "Substrate" defects can also gradually slip or climb up into the device volume to contribute to failure mechanisms.

Immediate effects

"Fatal" defects, device yields and good housekeeping Defects that cause the device to fail to perform within specification on first production are picturesquely described as fatal. These are generally large defects, so major effects are produced over a significant fraction of the area of the device, e.g., large precipitates producing excessively soft or premature reverse breakdown, diffusion pipes shorting through base layers, regions of slip at the edge of the wafer, etc. Fatal defects are a major factor determining the yield (the percentage of useable devices per slice processed). Yield strongly influences price competitiveness so the minimization of fatal defects is a primary objective of process development and quality control. Microcharacterization, together with a background knowledge of defect characteristics and the means by which they are introduced in growth and processing, is used to guide efforts to eliminate such defects. Often, in industry, problems "go away" due simply to applying what past experience showed to be good practice. Thus, the use of improved materials, tightening up on both cleanliness and the accuracy of control of process parameters, generally results in the necessary improvement in yield. Because this works so often and works quickly, many process engineers have little interest in semiconductor defect research.

Device performance limiting effects

Excess noise Dislocations introduce energy levels in the forbidden gap and can contribute to electrical noise (Brophy, 1956, 1959). Morrison (1956) also suggested charge controlled recombination at dislocations is responsible for carrier decay that is slower than predicted by Shockley-Read-Hall theory. Brophy (1956, 1959), and Conrad and Frederick (1966) studied the effect of dislocations in Si and Ge on 1/f noise. The latter authors found that the 1/f noise constant fell sharply with dislocation densities above 10^6 cm^{-2} in Ge. Yu *et al.* (1967) compared the 1/f and generation recombination noise in deformed and virgin samples of Si and concluded that the effects were due to generation and recombination at dislocation sites. Blasquez (1978) concluded, as the result of experiments on several dozen wafers, that crystallographic defects are the main source of burst noise. These properties would make dislocation densities above some threshold value unacceptable in devices requiring low noise such as detectors for weak signals.

Excess leakage currents Excessive leakage currents in devices are often blamed on defects. A problem in correlating leakage with defects is that the effectiveness of any defect is likely to depend strongly on the extent to which it is decorated by impurity atoms and on the nature of the impurity (e.g., Table 2). An example in which this problem did not arise is a part of some recent work by Hull and Bean and their co-workers on misfit dislocations in strained layer Ge_xSi_{1-x}/Si structures (for a review, see Hull and Bean, 1994). They found that relaxation by the gradual introduction of increasing densities of misfit dislocations could be observed by annealing the specimens in a TEM hot stage. Then they added a top and bottom contact to the specimen so that reverse bias leakage current could be measured in such specimens containing a p-n junction. Ross *et al.* (1993a,b) found that the reverse leakage current increased linearly with the dislocation density as shown in Figure 17 in a device with the layer thicknesses and doping concentrations shown in the insert (the density is measured by the standard method of counting the number of dislocations that cut a known length of randomly placed and oriented line and averaging several such values). This linear relation gave an effective current of $\approx 10^{-5}$ to 10^{-4} A/m of misfit dislocation line which was in good agreement with the value found by Bull *et al.* (1979) for densities of dislocations threading through Si bipolar transistor base-emitter junctions. Thus, dislocations in different situations produced at times fourteen years apart, had consistent effects. Ross *et al.* (1993a,b) showed by simple calculations that this leakage current per unit length would require a number of generation-recombination sites per unit length that was far too great to correspond to core sites. Therefore, they suggested that point defects around the dislocations or on the planes swept by the threading dislocations in extending the interfacial misfit dislocation segments must be involved.

Mechanisms of fatal defects in devices that have been studied in detail

A few fatal defects have been investigated in sufficient depth to reveal their mechanisms of operation.

Soft reverse characteristics in Si diodes In reverse biasing a diode, an increasing voltage is applied to drive current through a barrier and eventually some form of "breakdown" takes place. In well-made, uniform p-n junctions, this occurs over the whole area by a non-destructive process such as Zener tunneling, and only at relatively large and well-defined reverse biases. Defects can cause localized high current densities to flow "prematurely," i.e., at a lower voltage than that for uniform breakdown. Such behaviour is called soft breakdown. This often leads to "thermal run-away". That is, local heating makes the material more conductive so the current increases, increasing the heating and so on. This can end in melting and shorting the device or in catastrophic mechanical shattering in high power devices. The importance of such fatal defects and the appearance of several varieties of the phenomenon in different devices at different times resulted in a large body of published work on these phenomena.

Microplasma breakdown in power diodes was found to be correlated with dislocations. Soft reverse characteristics (current increasing gradually with reverse bias) in early Si diodes correlated with the appearance of light emitting spots at dislocation threading points (Chynoweth and Pearson, 1958). Figure 18 (from Chynoweth, 1960) shows patterns of luminescent spots on a diode; it can be seen that the luminescent spots are lined up along slip plane traces. Shockley (1961) suggested, on the basis of calculations, that this was not due to the dislocations themselves but to precipitates formed at the dislocations which acted as electric field concentrators. The practical solution to the problem, found by Goetzberger and Shockley (1961), was phosphorus glass "gettering" which removes the metal impurities that produce the precipitates. Later, Cullis and Katz (1974), using TEM, identified microplasma sites due to Fe silicide needle crystals at dislocations as the defect responsible for these phenomena.

The mechanism of microplasma (a localized region of high electron-hole density) luminescence is the acceleration of electrons by the high field. The electrons reach energies lying high in the conduction band from which they relax to lower conduction band states by photon emission. These **intraband** transitions can be of higher (visible) energies than the conduction to valence **interband** transitions, which emit photons only in the lower energy infrared region (Newman, 1955).

Other types of defect can also cause failure in Si diodes under reverse bias. For example, Roy (1971) found that hot-spot failures in the epitaxially grown diodes made in his firm, at that time, never occurred at dislocation or stacking fault sites, only at larger defects (tripyramids, raised-triangles or hexagons) which were due to contamination of the substrate surface.

Ravi *et al.* (1973) carried out an important early study of oxidation induced stacking faults (OISFs) which introduce excess reverse leakage currents in Si diodes. The effect of the OISFs varied considerably. TEM showed them to be precipitate decorated, especially at the bounding partial dislocations. Ravi *et al.* (1973) used EBIC to determine the electrical activity of individual OISFs and found that this depended on the amount of decoration present and on the size of the fault, i.e., the depth to which it penetrated relative to the p-n junction.

A related phenomenon is microplasma breakdown in avalanche photo diodes (APDs). These Si infrared photodetectors are diodes that can be designed to operate under hundreds of volts reverse bias so that the depletion region of the p-n junction widens to "reach through" the whole thickness of the Si slice (such APDs are called reach-through avalanche photodiodes). Thus, a large volume of material is subjected to large, near-breakdown fields that cause avalanche multiplication of the carriers generated by the absorbed infrared photons. In avalanche multiplication, electrons are accelerated to gain energy well above the thermal equilibrium value. These so-called hot electrons become energetic enough to generate hole-electron pairs by ionizing collisions with the lattice. The two electrons are then accelerated to generate more carriers and so on. The result is described as an "avalanche" of carriers. Rejection of the devices is often due to noisy breakdown of the diodes at voltages below the designed operating bias. That is, premature localized breakdown occurs before reaching the bias voltage required to give the large current pulse avalanche triggered by one absorbed photon for which the device was designed.

This phenomenon was studied by Lesniak and Holt (1983, 1987), and Holt and Lesniak (1985). They used EBIC and found that the devices contained large numbers of diffusion induced misfit dislocations which could be seen with no bias applied as in Figure 19a. On applying reverse biases just less than breakdown values, the local avalanche microplasma sites appeared as bright EBIC spots (Fig. 19b). The reason is that the site is held at a bias just below the local breakdown value and the arrival of the beam at that point stimulates the onset of avalanching, producing a high current detected as a strong EBIC signal.

Lesniak (Lesniak and Holt, 1987) showed that this could be exploited to measure the properties of indivi-

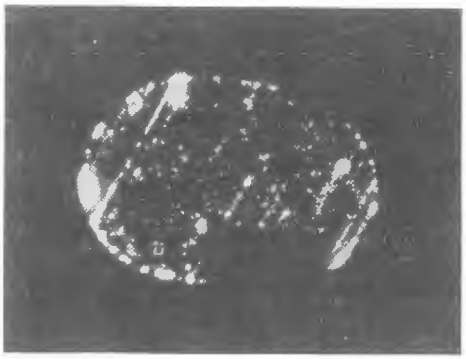

Figure 18. Luminescent microplasma breakdown sites in a reverse biased Si p-n junctions appear as bright points aligned along slip plane traces (after Chynoweth, 1960).

---

dual microplasmas by recording EBIC linescans across such sites at a series of increasing biases passing through the breakdown value. Figure 20 is a microplasma scan for a bias just below breakdown. When the beam was incident on the microplasma site, it gave the high steady current value producing the peak in the profile. When the beam was incident elsewhere, thermal fluctuations generated carriers at random times to precipitate single bursts of avalanche current. Consequently, the microplasma current switching on and off produced the high noise recorded over the rest of the scan. This form of noise is characteristic. Lesniak's quantitative results were in good agreement with theory (Lesniak and Holt, 1987).

The conclusion of the study was that neither dislocations nor precipitates were responsible for microplasmas in the APDs. It is due to dislocation retarded diffusion which results in the p-n junction being much less deep below the dislocations (Fig. 21). The sharp cusps in the junction act to concentrate the field and allow localized premature breakdown. It can be seen in Figure 19b that the dislocations occur in bright strips due to high-efficiency charge collection above the cusps where the p-n junction rises toward the hole-electron pair generation volume near the top surface.

High power thyristors are another type of device in which large volumes of Si are subjected to large voltages. Again, disastrous breakdown can occur at localized points. Such hot spots sometimes form at well below the designed operating voltage. Hill *et al.* (1975) showed that this occurred at the sites of a type of large defect that could often be shown to have arisen from defect-related stress centers that were present in the starting material. Subsequently, it appeared that this was correlated with the probable presence of hydrogen in the material so this was probably a case of breakdown

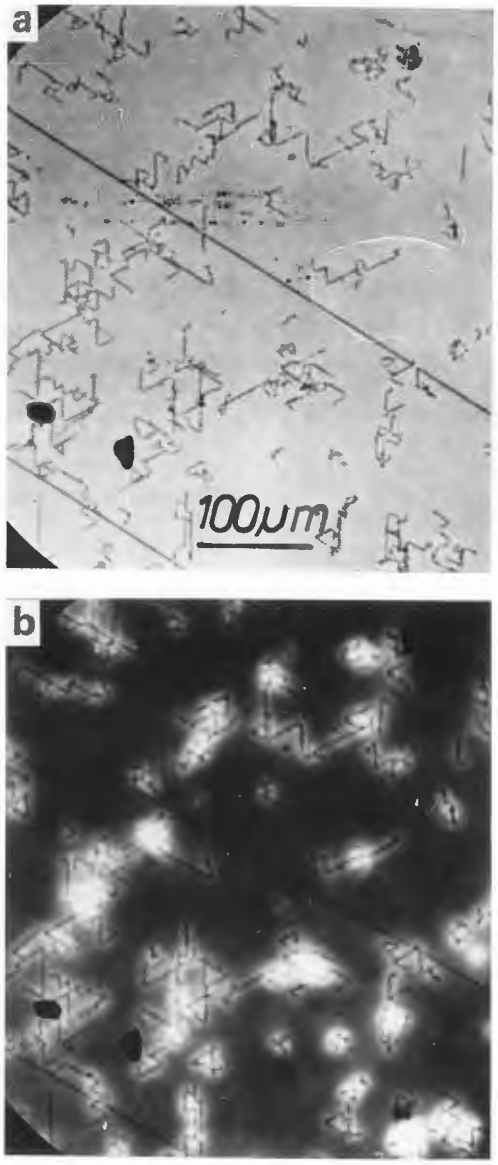

Figure 19. EBIC micrographs of a Si avalanche photodiode (APD) under (a) zero and (b) 266 V reverse bias. The fine zig-zag dark lines in (a) are bits of a network of diffusion-induced misfit dislocations. Microplasma sites appear as bright spots in (b) and it can be seen that they are associated with the dislocations and especially with nodal points in the network. (After Holt and Lesniak 1985).

---

through bubbles at defect sites.

For a review of early material problems in silicon power devices see John (1967).

Related device phenomena

Schwuttke (1970), working in industry, carried out systematic X-ray topographic studies of defects in pro-

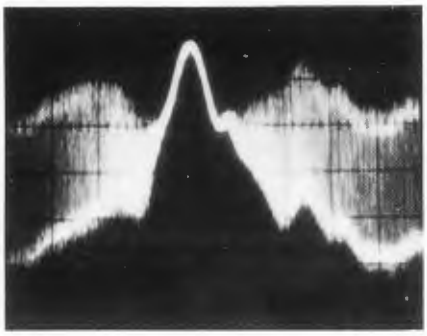

Figure 20. EBIC linescan recorded across a microplasma site in an APD held at just less than the breakdown bias required to turn it steadily on. When the beam hits the site it turns it on giving the smooth EBIC current peak. When the beam is incident elsewhere, thermal fluctuations trigger brief random avalanches of carriers producing the high noise recorded over the rest of the scan. (After Holt and Lesniak, 1985).

---

cessed Si and gave a review which lists many references on the role of dislocation decoration in devices.

Changes in n-p-n transistor parameters including soft junction breakdown were found to correlate with increasing gold concentrations in the base regions when dislocations were present (Parekh, 1971). This paper gives references to several other device effect studies.

Defects and Accelerated Device Failure Mechanisms

An important mode of rapid failure in early GaAs based DH (double heterostructure) lasers was that due to dark line defects (DLDs). These defects were resolvable in infrared microscopy (Fig. 22a) and grew rapidly during laser operation (Johnston and Miller, 1973). TEM studies showed the DLDs were tangles of dislocation dipoles and loops (Fig. 22b). These climbed rapidly out of dislocations threading the active layer due to recombination enhanced dislocation climb possibly by the "phonon kick" mechanism (Petroff and Hartman, 1973, 1974). A similar mechanism was also found to operate in LEDs (Petroff *et al.*, 1976), especially in those that require large current densities for their operation as we shall see. For a review of defects and degradation of III-V optoelectronic devices see Ueda (1988).

Unlike the GaAs based devices, InP based lasers do not experience DLD failure. The reason for this is not known but see the comments on InP-based LEDs below.

Chin (1984) published a review of studies of the effects of dislocations and other defects in three types of LEDs which are summarized below:

(1). In graded-band gap GaAlAs LEDs, CL revealed threading dislocations as dark dots. Roedel *et al.* (1979) then found the luminescent efficiency of these light-emitting diodes to vary with the density of such threading dislocations extending up from the substrate as shown by the open circles in Figure 23. They treated the effect of the dislocations on the diffusion of the injected carriers, assuming that the dislocations were perpendicular to the p-n junction and could be represented as having infinite recombination velocity. They obtained, for the relation between the quantum efficiency, η, of the LED and the dislocation density, ρ:

$$\eta/\eta_0 = (1 + \pi^2 L^2 \rho)^{-1} \qquad (26)$$

where η_0 is the efficiency of a dislocation-free diode. Results for the 45 diodes plotted in Figure 23 fit quite well the curve of eq. (26) for $\eta_0 = 6.5\%$ and $L = 11.0$ μm showing that the dislocation density controlled the efficiency in these devices for densities above about $\rho = 10^3$ cm^{-3}. (This curve was included in Figure 2).

The dislocation content, however, had no influence on the mean time to failure which Chin ascribed to the low operating current density of these devices. This would mean that the accelerated climb mechanism whereby DLDs (dark line defects) grow from threading dislocations would be ineffective. Diodes from some wafers, however, did undergo accelerated failure under test by the DLD mechanism. Examination showed that these devices had Si-rich (Si was a dopant used) pyramid-shaped protrusions on their top surfaces and <110> dislocation networks grew from the pyramids. When the dislocations reached the p-n junction they became effective and appeared as DLDs in the electroluminescence images.

(2). Restricted contact (stripe geometry) double heterostructure GaAlAs LEDs operate at high current densities (36 kA/cm^2) and Chin *et al.* (1980) showed that threading dislocations appeared as dark spots and acted as sources for DLD rapid failure (within 20 hours at 6 kA/cm^2 and 25°C). To avoid these problems, low dislocation density ($< 10^3$ cm^2) highly Si-doped GaAs substrates were used. Substrate surface contamination and supercooling during growth were identified as causing the incorporation of stacking faults and dislocation networks, respectively, in the GaAlAs.

(3). Restricted contact, double heterostructure InP/InGaAsP LEDs were found to be exceptionally reliable because the performance is relatively insensitive to structural defects. The mean time to failure (MTTF) was estimated to be $\geq 10^9$ hours at 60°C (Yamakoshi *et al.*, 1981; Zipfel *et al.*, 1983). However, even in these LEDs, the effects on performance and reliability of threading and misfit dislocations and indium-rich in-

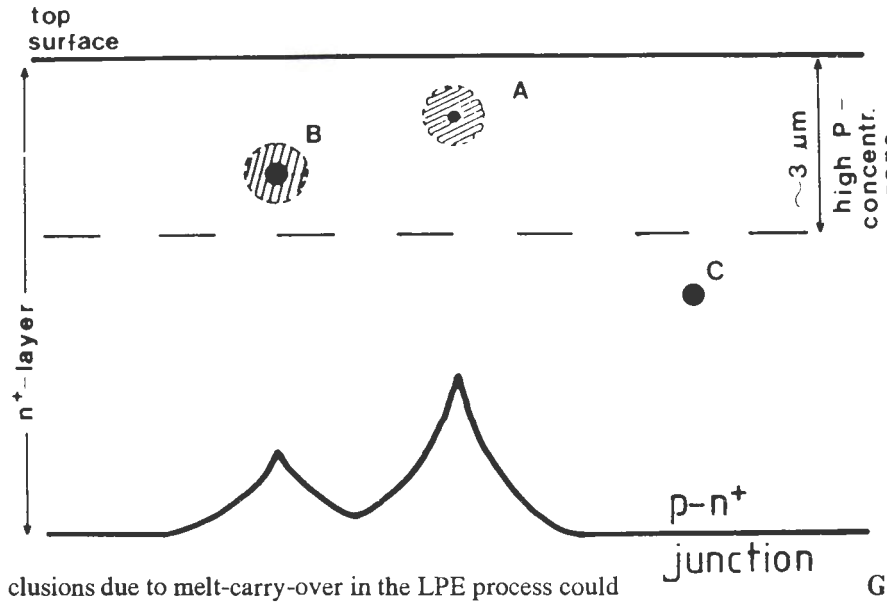

Figure 21. Schematic diagram illustrating the way in which diffusion induced dislocations like those shown at A and B, by absorbing the diffusing impurity, retard the diffusion front and produce cusps in the p-n junction. The magnitude of the effect depends on the depth of the dislocation. Shallower ones produce the larger effect. Microplasma breakdown occurs at the field-concentrating cusps it is believed. (After Lesniak and Holt, 1987).

clusions due to melt-carry-over in the LPE process could be studied. The threading dislocations did not significantly affect device performance or reliability although they acted as non-radiative recombination centers. Chin (1984) explained this by the recombination rate at such dislocations in InP being lower than that in GaAs as exemplified by their poorer contrast in luminescence micrographs (Maeda and Takeuchi, 1981). Moreover, TEM studies showed that the rate of growth of dipole dislocations (DLDs) from threading dislocations in these diodes is low for typical device operating conditions (10^{-10} cm/s at 50°C compared to 10^{-4} to 10^{-7} cm/s in GaAs; Ishida *et al.*, 1982). The weak influence of misfit dislocation networks on device performance was ascribed by Chin (1984) to the fact that they occur in the p-InP confining layer, not the active layer. They do have an effect on reliability but only after 10^4 hours at a high current density (40 kA/cm^2). This, Chin (1984) ascribed to the fact that they have to propagate into the active layer to affect the device (their electroluminescence contrast was observed to increase from ~ 5% to ~ 50% as a result). In addition to threading dislocations, the InP substrates contained the characteristic defects known as grappes (French for bunches of grapes). These appear as clusters of pits when the surface is etched and are due to numerous dislocations thrown out by prismatic punching from inclusions which are possibly gas bubbles (Elliott and Regnault, 1981; Augustus and Stirland, 1982). These were found to be harmful if located near the substrate surface as they could give rise to numerous threading dislocations in the epilayers or to growth hillocks.

For full references to the literature on all these topics, see Chin (1984).

Green and Blue LEDs

At present, there is competition to develop economical green and blue emitting semiconductor LEDs and lasers. The two new competitive materials technologies are II-VI (ZnSe) based and III-V nitride (GaN) based (SiC blue LEDs have been available for some years). For reviews of recent work directed to the development of blue-green semiconductor lasers, see Neu ...ик *et al.* (1994), and Luo and Furdyna (1995). One fact affecting the competition between the two new materials systems is that the II-VI devices are subject to DLD failure (Gunshor and Nurmikko, 1995) whereas the GaN LEDs at least are not (Cook and Schetzina, 1995). The latter authors ascribe this difference to the greater hardness of GaN.

It would be difficult to explain it simply in terms of eq. (26). This would require that the value of L be small enough to compensate the large value of ρ in GaN. However,

$$L = (D\tau)^{1/2} \qquad (27)$$

where D is the diffusion coefficient and τ is the minority carrier lifetime; and

$$\{1/\tau\} = \{[1/\tau_{nr}] + [1/\tau_r]\} \qquad (28)$$

where τ_{nr} and τ_r are the non-radiative and radiative recombination times respectively. Hence, the excessively small value of L that would be required to render the several orders-of-magnitude higher value of ρ ineffective would require that τ_r and τ_{nr} also be exceedingly small. This small value of τ_r means the luminescent efficiency would be correspondingly large. That is, this line of argument amounts to saying that the dislocations in GaN

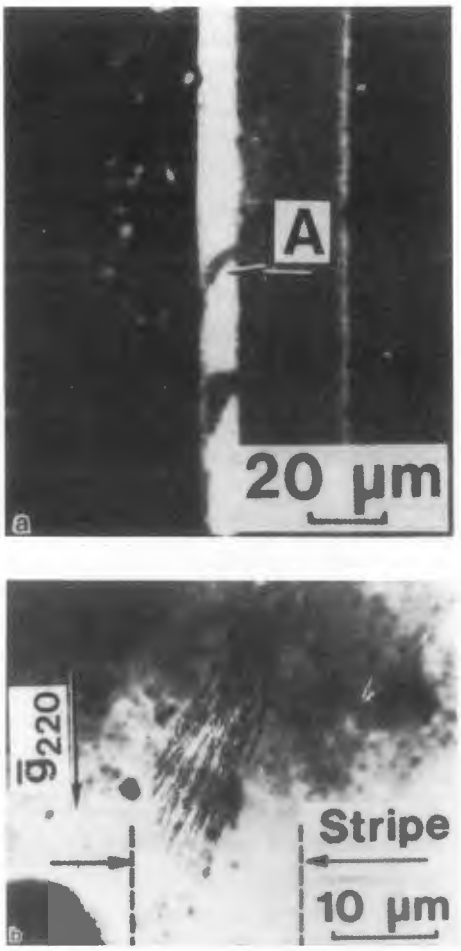

Figure 22. (a) Infrared electroluminescence image of a rapidly degraded GaAlAs/GaAs double heterostructure (DH) laser showing <100> oriented dark line defects (DLDs) crossing the active laser stripe, for example, at position A. (b) Transmission electron micrograph showing the dislocation network corresponding to the DLDs shown in (a). (After Ueda, 1988).

---

are not effective because their presence is not sufficient to compensate the enormous luminescent efficiency of the material. Such an efficiency seems unlikely. It is more likely that the infinite recombination at the dislocations assumed in deriving eq. (26) does not apply, as Cook and Schetzina (1995) suggested.

Activation energies for modes of silicon device failure

We have reviewed the few cases in which the mechanisms of defect-related failure modes have been studied in some detail for particular cases of a device-processing technology-material combination. Of course, there have been many cases of materials characterization in the device industry that have revealed defects and thrown some

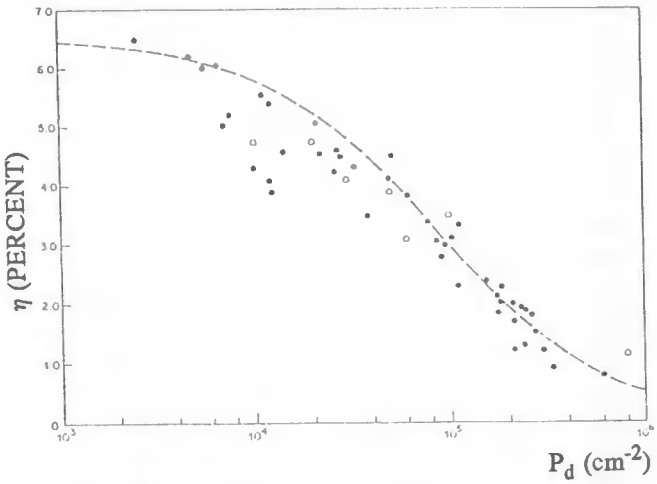

Figure 23. Plots of measured luminescent efficiency versus the density of dislocations threading through forty five $Ga_{1-x}Al_xAs$:Si LEDs (solid circles) or the density of dislocations in the substrate determined by etching (open circles). The dashed line is the plot of eq. (26) for η_o = 6.5% and L = 11.0 μm. (After Roedel *et al.*, 1979).

---

light on their role in yield and failure. This is especially the case for the microelectronics industry. See, for example, the books of Ravi (1981), and Marcus and Sheng (1983) (listed in **Appendix I**) and the reviews by, e.g., John (1967), Schwuttke (1970), and Cerva (1991) (listed in **Appendix II**).

Additional information is constantly generated by failure analyses (see the many examples in the book of Richards and Footner, 1992, listed in **Appendix I**) and by accelerated life testing for reliability improvement. Life testing yields values of activation energies for the many different failure modes. A table of such data was drawn up by Dr. B.P. Richards (GEC-Marconi Materials Technology, Hirst Division, Elstree Way, Boreham Wood, Herts., WD6 1RX, U.K.) from the relatively little published literature and the unpublished results of testing at a number of major British Centers. He listed 195 values for silicon devices grouped under headings ranging from electromigration in several forms of metallization through Al-Ti silicide interaction and other alloying reactions to mechanical defects, i.e., fractures, shorts, etc. Included were nine entries under the heading of Si crystal defects generally not further described. This is quoted to indicate the rich variety of modes of failure, differing from device to device, and with type of metallization etc. which is constantly being encountered. They are rarely investigated in detail because neither the time nor the funding is available. Clearly, there is still much to be learned.

The Importance of Scanning Beam Methods and the Need for Systematic Device Defect Research

Just as for basic studies, so for device effect studies, it is desirable for understanding to move on from the effects of plastic deformation to those of individual defects. Many defects can be present and have no effect either because they miss the active regions of small devices or because they are insufficiently dirty (e.g., no precipitates present) (Holt, 1979). The magnitude of an effect per defect can change with time apparently due to cleaner technology leading to less heavily decorated defects (e.g., the data in Table 2). Scanning beam methods can overcome these problems by locating for study individual defects known to be electrically active by EBIC or LBIC or known to be optically active in the device by CL or scanned laser beam PL and whose type and state of decoration can be determined. Thus, the use of scanning beam methods can also make a powerful contribution to device studies.

Possible Device Benefits of Dislocations and Their Failure in Application

Many suggestions have been made over the years to employ defects to produce or enhance device functions. All have failed to reach the market.

An early device proposal was the grain boundary transistor (Matare, 1955, 1956). There were often impurity-segregation layers at grain boundaries of type opposite to that of the material (e.g., p-type boundary layers between n-type grains). The suggestion was that contacts be made to each of the grains and to the boundary to produce an n-p-n transistor. Photosensors were proposed based on the photovoltaic response of grain boundaries in Ge and Si (Mueller, 1959) and in InSb (Mueller and Jacobson, 1959).

A reduction in minority carrier lifetime can be produced by recombination at dislocations (Fig. 1). It was proposed that this should be used to reduce device switching times by introducing dislocations (Pearson and Riesz, 1959). However, in addition, deformation produces complex, interrelated effects, introducing both a fast recombination and a slow trapping time as well as a reduction in carrier density (Neubert *et al.*, 1973). It was found that the turn-off delay of a Ge npn mesa transistor could be reduced by plastic deformation (Schumann and Rideout, 1964).

A major reason that none of these proposals were adopted in practice is the difficulty of producing well-defined dislocation structures sufficiently controllably or reproducibly to be a viable production technique.

Recently, Rozgonyi *et al.* (1987) argued, however, that interfacial misfit dislocations constitute a case in which the depth and density of the dislocations can be controlled. Radzimski *et al.* (1991) showed that the electrical activity of such misfit dislocations is strongly dependent on the type and amount of impurity which decorates them (Au at misfit dislocations in Si/SiGe/Si interfaces). Such gold-decorated dislocations were intentionally placed within the space charge layer of a power diode and shown to enhance its switching properties. So it is still possible that device applications of dislocations could appear in practice.

Conclusions

We are now well on our way toward a basic understanding of the properties of defects, especially dislocations and grain boundaries in some semiconducting materials. For an introduction to the grain boundary literature see the proceedings of the Polycrystalline Semiconductor Conferences, e.g., Strunk *et al.* (1994) (listed in **Appendix I**). Device effects represent interesting examples of more complex situations in which defects can occur, e.g., in the presence of space charge layers in p-n junction (and other barrier) depletion regions, in high field regions in APDs and in the high densities of photons in the active layers of lasers. Hence, interesting new defect-related physical phenomena can be encountered and need to be studied. The combination of spatial resolution with analytical capability of scanning beam methods is needed to analyse device effect phenomena and much remains to be clarified. A striking example is the puzzle presented by the new bright blue GaN Nichia LEDs. How is it that these show high luminescence efficiency despite the presence of 10^{10} dislocations cm^{-2} when GaP and GaAs LEDs cannot function with more than 10^4 or 10^6 dislocations present per cm^2 (see Fig. 2 and the discussion thereof)?

Suggestions for Further Reading

Topics covered in this review have been the subject of several good books and proceedings (**Appendix I**) and useful recent review articles (**Appendix II**). Some of the citations in these sections are also included in **References**.

Appendix I. Reviews of the Properties of Defects in Semiconducting Materials and Devices: Books

Marcus RB, Sheng TT (1983) Transmission Electron Microscopy of Silicon VLSI Circuits and Structures. Wiley-Interscience, New York.

Ravi KV (1981) Imperfections and Impurities in

Semiconductor Silicon. Wiley, New York.

Richards BP, Footner PK (1992) The Role of Microscopy in Semiconductor Failure Analysis. Oxford University Press, Oxford, U.K.

Important Proceedings series, Recent volumes in:

The BIADS Conferences: Beam Injection Assessment of Defects in Semiconductors, 1993. Mat. Sci. Eng. **B24** (1994) No. 1-3.

The DRIP Conferences (honest!): Defect Recognition and Image Processing in Semiconductors and Devices, 1993. Conf. Series No. 135 (Inst. Phys., Bristol).

The ICDS Conferences: Proc. 16th. International Conference on Defects in Semiconductors (Lehigh University, Bethlehem, Pennsylvania) (1991).

The MSM Meetings: Microscopy of Semiconducting Materials, 1993. Conf. Series No. 134 (Inst. Phys., Bristol).

The PS Meetings: Strunk HP, Werner JH, Fortin B, Bonnaud O (eds.) (1994) Polycrystalline Semiconductors III - Physics and Technology. Sol. State Phenomena **37-38**. Scitec Publ., Zurich, Switzerland.

The SPDS Symposia: Proc. Seventh Internat. Symp. on Structure and Properties of Extended Defects in Semiconductors, 1992. Phys. Stat. Sol. **A138** (1993) No. 2.

Appendix II. Reviews of the Properties of Defects in Semiconducting Materials and Devices: Reviews

Alexander H (1986) Dislocations in semiconductors. In: Dislocations in Solids. Vol. 7. Nabarro FRN (ed.). North-Holland, Amsterdam. pp. 113-234.

Alexander H (1991) Dislocations in semiconductors. In: Polycrystalline Semiconductors II. Werner JJ, Strunk HP (eds.). Springer-Verlag, Berlin. pp. 2-12.

Alexander H (1994) What information on extended defects do we obtain from beam-injection methods? Mat. Sci. Eng. **B24**, 1-7.

Bardsley W (1960) The electrical effects of dislocations in semiconductors. Prog. Semicond. **4**, 155-203.

Bullough R, Newman RC (1963) The interaction of impurities with dislocations in silicon and germanium. Prog. Semicond. **7**, 99-134.

Cerva H (1991) TEM materials characterization in Si technology. In: Microscopy of Semiconducting Materials 1991. Inst. Phys. (Bristol) Conf. Series **117**, 155-164.

Chin AK (1984) The effect of crystal defects on device performance and reliability. J. Cryst. Growth **70**, 582-596.

Figielski T (1978) Recombination at dislocations. Sol. State Electron. **21**, 1403-1412.

Hirsch PB (1981) Electronic and mechanical properties of dislocations in semiconductors. In: Defects in Semiconductors. Proc. Materials Res. Soc. 1980. North-Holland, New York. pp. 257-271.

Hirsch PB (1985) Dislocations in semiconductors. Mat. Sci. Tech. **1**, 666-677.

Holt DB (1979) Device effects of dislocations. J. de Phys. Colloque **C6**, 189-199.

John HF (1967) Silicon power device material problems. Proc. IEEE **55**, 1249-1271.

Labusch R, Schroter W (1978) Electrical properties of dislocations in semiconductors. In: Dislocations in Solids. Vol. 5. Nabarro FRN (ed.). North-Holland, Amsterdam. pp. 127-191.

Schwuttke GH (1970) Silicon material problems in semiconductor device technology. Microelectron. Reliability **9**, 397-412.

Ueda O (1988) Degradation of III-V opto-electronic devices. J. Electrochem. Soc. **135**, 11C-22C.

van Bueren HG (1960) Plastic deformation and the electrical properties of germanium and silicon. In: Imperfections in Crystals. North-Holland, Amsterdam. pp. 633-642.

Weber J (1994) Correlation of structural and electronic properties from dislocations in semiconductors. In: Polycrystalline Semiconductors III. Strunk HP, Werner JH, Fortin B, Bonnaud O (eds.). Scitec Publ., Zurich, Switzerland. pp. 13-24.

References

Alexander H (1986) Dislocations in semiconductors. In: Dislocations in Solids. Vol. 7. Nabarro FRN (ed.). North-Holland, Amsterdam. pp. 113-234.

Alexander H (1991) Dislocations in semiconductors. In: Polycrystalline Semiconductors II. Werner JJ, Strunk HP (eds.). Springer-Verlag, Berlin. pp. 2-12.

Alexander H (1994) What information on extended defects do we obtain from beam-injection methods? Mat. Sci. Eng. **B24**, 1-7.

Alexander H, Teichler H (1991) Dislocations. In: Materials Science and Technology, Vol. 4: Electronic Structure and Properties of Semiconductors. Schroter W (ed.). VCH, Weinheim, Germany. pp. 249-319.

Alexander H, Labusch R, Sander W (1965) Electron spin resonance in deformed silicon crystals. Sol. State Commun. **3**, 357-360.

Augustus PD, Stirland DJ (1982) A study of inclusions in indium phosphide. J. Electrochem. Soc. **129**, 614-621.

Bardsley W (1960) The electrical effects of dislocations in semiconductors. Prog. Semicond. **4**, 155-203.

Bell RL, Willoughby ARF (1966) Etch-pit studies of

dislocations in InSb. J. Mater. Sci. **1**, 219-228.

Bell RL, Willoughby ARF (1970) The effect of plastic bending on the electrical properties of indium antimonide 2. Four-point bending of n-type material. J. Mater. Sci. **5**, 198-217.

Bell RL, Latkowski R, Willoughby ARF (1966) The effect of plastic bending on the electrical properties of indium antimonide. J. Mater. Sci. **1**, 66-78.

Blasquez G (1978) Excess noise sources due to defects in forward biased junctions. Sol. State Electron. **21**, 1425-1430.

Booyens H, Vermaak JS, Proto GR (1977) Dislocations and the piezoelectric effect in III-V crystals. J. Appl. Phys. **48**, 3008-3013.

Booyens H, Vermaak JS, Proto GR (1978a) The piezoresistance effect and dislocations in III-V compounds. J. Appl. Phys. **49**, 1149-1155.

Booyens H, Vermaak JS, Proto GR (1978b) The anisotropic carrier mobility due to dislocations in III-V compounds. J. Appl. Phys. **49**, 1173-1176.

Breitenstein O (1989) Scanning DLTS. Rev. de Phys. Appl. Suppl C6. pp. C6-101 to C6-110.

Breitenstein O, Heydenreich J (1985) Review. Scanning deep level spectroscopy. Scanning **7**, 273-289.

Brophy JJ (1956) Excess noise in deformed germanium. J. Appl. Phys. **27**, 1383-1384.

Brophy JJ (1959) Crystalline imperfections and 1/f noise. Phys. Rev. **115**, 1122-1125.

Broudy RM (1963) The electrical properties of dislocations in semiconductors. Adv. Phys. **12**, 135-184.

Brummer O, Schreiber J (1974) Zum lumineszenzverhalten von versetzungen in CdS-einkristallen (On the luminescence properties of dislocations in CdS single crystals). Kristall Technik **9**, 817-829.

Brummer O, Schreiber J (1975) Mikroskopische kathodolumineszenzuntersuchungen an halbleitern mit der elektronenstrahlmikrosonde (Microscopic cathodoluminescence investigations on semiconductors with the electron microprobe). Microchimica Acta **Suppl. 6**, 331-344.

Bull C, Ashburn P, Booker GR, Nicholas KH (1979) Effects of dislocations in silicon transistors with implanted emitters. Sol. State Electron. **22**, 95-104.

Bullough R, Newman RC (1963) The interaction of impurities with dislocations in silicon and germanium. Prog. Semicond. **7**, 99-134.

Canham LT, Dyball MR, Barraclough KG (1989) Surface copper contamination of As-received float-zone silicon wafer. J. Appl. Phys. **66**, 920-927.

Castaldini A, Cavallini A (1989) Imaging of extended defects by quenched infra-red beam induced currents (Q-IRBIC). In: Point and Extended Defects in Semiconductors. Benedek G, Cavallini A, Schroter W (eds.). Plenum Press, New York. pp. 257-268.

Castaldini A, Cavallini A, Gondi P (1987) IRBIC semiconductor defect pictures. Bull Acad Sci USSR Phys **51**, 77-80.

Cavallini A, Castaldini A (1991) Developments of IRBIC and QIRBIC in defect studies: A review. J. de Phys. Colloque **C6**, 89-99.

Chin AK (1984) The effect of crystal defects on device performance and reliability. J. Cryst. Growth **70**, 582-596.

Chin AK, Keramidas VG, Johnston WD, Mahajan S, Roccasecca DD (1980) Evaluation of defects and degradation in GaAs-GaAlAs wafers using transmission cathodoluminescence. J. Appl. Phys. **51**, 978-983.

Chynoweth AG (1960) Internal field emission. In: Progress in Semiconductors **4**, 95-123.

Chynoweth AG, Pearson GL (1958) Effect of dislocations on breakdown in silicon p-n junctions. J. Appl. Phys. **29**, 1103-1110.

Claesson A (1979) Effect of disorder and long range strain field on the electron states. J. de Phys. Colloque **C6**, 39-41.

Conrad H, Frederick S (1966) The effect of dislocation density on 1/f noise in germanium. Mat. Sci. Eng. **1**, 141-143.

Cook JW, Schetzina JF (1995) Blue-green light-emitting diodes promise full-color displays. Laser Focus World (March), 101-104.

Cullis AG, Katz LE (1974) Electron microscope study of electrically active impurity precipitate defects in silicon. Phil. Mag. **30**, 1419-1443.

Donolato C (1978/1979) On the theory of SEM charge-collection imaging of localized defects in semiconductors. Optik **52**, 19-36.

Donolato C (1985) Beam induced current characterization in polycrystalline semiconductors. In: Polycrystalline Semiconductors. Physical Properties and Applications. G Harbeke (ed.). Springer-Verlag, Berlin. pp. 138-154.

Duesbury MS, Richardson GY (1991) The dislocation core in crystalline materials. CRC Crit. Rev. Sol. State. Phys. Mater. Sci. **17**, 1-46.

Elliott CR, Regnault JC (1981) Birefringence studies of defects in III-V semiconductors. In: Microscopy of Semiconducting Materials 1981. Inst. Phys. (Bristol) Conf. Series No. 60. pp. 365 -370.

Fell TS, Wilshaw PR (1989) Recombination at dislocations in the depletion region in silicon. In: Structure and Properties of Dislocations in Semiconductors 1989. Inst. Phys. (Bristol) Conf. Series No. 104. pp. 227-232.

Fell TS, Wilshaw PR (1991) Quantitative EBIC investigation of deformation-induced and copper decorated dislocations in silicon. In: Microscopy of Semiconduct-

ing Materials 1991. Inst. Phys. (Bristol) Conf. Series No. 117. pp. 733-736.

Fell TS, Wilshaw PR, de Coteau MD (1993) EBIC investigations of dislocations and their interactions with impurities in silicon. Phys. Stat. Sol. **A138**, 695-704.

Figielski T (1978) Recombination at dislocations. Sol. State Electron. **21**, 1403-1412.

Galloway SA, Wilshaw PR, Fell TS (1993) An EBIC investigation of alpha, beta and screw dislocations in gallium arsenide. In: Microscopy of Semiconducting Materials 1993. Inst. Phys. (Bristol) Conf. Series No. 134. pp. 71-76.

Goetzberger A, Shockley W (1960) Metal precipitates in silicon p-n junctions. J. Appl. Phys. **31**, 1821-1824.

Grazhulis VA (1979) Application of EPR and electric measurements to study dislocation energy spectrum in silicon. J. de Phys. Colloque **C6**, 59-61.

Gunshor RL, Nurmikko AV (1995) Blue-green laser-diode technology moves ahead. Laser Focus World (March), 97-100.

Heggie MI, Jones R, Lister GMS, Umerski A (1989) Interaction of impurities with dislocation cores in silicon. In: Structure and Properties of Dislocations 1989. Inst. Phys. (Bristol) Conf. Series No. 104. pp. 43-46.

Hergert W, Pasemann L (1984) Theoretical study of the information depth of the cathodoluminescence signal in semiconductor materials. Phys. Stat. Sol. **a85**, 641-648.

Higgs V, Kittler M (1993) Investigation of recombination at misfit dislocations in SiGe CVD structures by 1:1 correlation of EBIC and CL. In: Microscopy of Semiconducting Materials 1993. Inst. Phys. (Bristol) Conf. Series No. 134. pp. 703-706.

Higgs V, Kittler M (1995) The influence of hydrogen, oxygen and transition metal contamination on the optical and electrical activity of dislocations in bulk Si and SiGe. In: Microscopy of Semiconducting Materials 1995. Inst. Phys. (Bristol) Conf. Series. No. 146. pp. 723-728.

Higgs V, Lightowlers EC (1992) Characterization of extended defects in Si and Si_{1-x} Ge_x alloys: The influence of transition metal contamination. Materials Res. Soc. Symp. Proc. **263**, 305-316.

Higgs V, Lightowlers EC, Davies G, Schaffler F, Kasper E (1989) Photoluminescence from MBE Si grown at low temperatures; donor bound excitons and decorated dislocations. Semicond. Sci. Technol. **4**, 593-598.

Higgs V, Lightowlers EC, Kightley P (1990a) Dislocation related d-band luminescence: The effects of transition metal contamination. Materials Res. Soc. Symp. Proc. **163**, 57-62.

Higgs V, Norman CE, Lightowlers EC, Kightley P (1990b) Characterization of clean dislocations and the influence of transition metal contamination. Vol. 1. Proc. 20th Conf. on the Phys. of Semicond. Stassanakis EM, Joannepoulos JD (eds.). World Scientific, Singapore, pp. 706-709.

Higgs V, Norman CE, Lightowlers EC, Kightley P (1991) Characterization of dislocations in the presence of transition metal contamination. In: Microscopy of Semiconducting Materials 1991. Inst. Phys. (Bristol) Conf. Series No. 117. pp. 737-742.

Higgs V, Lightowlers EC, Norman CE, Kightley P (1992) Characterization of dislocations in the presence of transition metal contamination. Mat. Sci. Forum **83-87**, 1309-1314.

Hill MJ, van Iseghem PM, Sittig R, Popp G (1975) Localized homogeneity problems for high-power thyristors. In: Inst. Phys. (Bristol) Conf. Series No. 23. pp. 522-530.

Hirsch PB (1981) Electronic and mechanical properties of dislocations in semiconductors. In: Defects in Semiconductors. Proc. Materials Res. Soc. 1980. North-Holland, New York. pp. 257-271.

Hirsch PB (1985) Dislocations in semiconductors. Mat. Sci. Tech. **1**, 666-677.

Hornstra J (1958) Dislocations in the diamond lattice. Phys. Chem. Solids **5**, 129-141.

Holt DB (1979) Device effects of dislocations. J. de Physique Colloque **C6**, 189-199.

Holt DB (1989) The conductive mode. In: SEM Microcharacterization of Semiconductors. Holt DB, Joy DC (eds.). Academic Press, London. Chapter 6.

Holt DB (1994) Local grain boundary property measurements. In: Polycrystalline Semiconductors III. Strunk HP, Werner JH, Fortin JB, Bonnaud O (eds.). Scitec Publ., Zurich, Switzerland. pp. 171-182.

Holt DB, Lesniak M (1985) Recent developments in electrical microcharacterization using the charge collection mode of the scanning electron microscope. Scanning Electron Microsc. **1985**, 67-86.

Hull R, Bean J (1994) *In situ* observations of misfit dislocations in lattice-matched epitaxial semiconductor heterostructures. Materials Res. Soc. Bulletin (Sept.), 32-37.

Ishida K, Kamejima T, Matsumoto Y, Endo K (1982) Lattice defect structure of degraded InGaAsP-InP double-heterostructure lasers. Appl. Phys. Lett. **40**, 16-17.

Jakubowicz A (1986) Theory of cathodoluminescence contrast from localized defects in semiconductors. J. Appl. Phys. **59**, 2205-2209.

John HF (1967) Silicon power device material

problems. Proc. IEEE **55**, 1249-1271.

Johnston WD, Miller BI (1973) Degradation characteristics of CW optically pumped $Al_xGa_{1-x}As$ heterostructure lasers. Appl. Phys. Lett. **23**, 192-194.

Jones R (1979) Theoretical calculations of electron states associated with dislocations. J. de Phys. Colloque **C6**, 33-38.

Jones R, Umerski A, Stitch P, Heggie MI, Oberg S (1993) Density-functional calculations of the structure and properties of impurities and dislocations in semiconductors. Phys. Stat. Sol. **A138**, 369-381.

Kittler M, Seifert W (1981) On the sensitivity of the EBIC technique as applied to defect investigations in silicon. Phys. Stat. Sol. **A66**, 573-583.

Kittler M, Seifert W (1993a) On the origin of EBIC defect contrast in silicon: A reflection on injection- and temperature-dependent investigations. Phys. Stat. Sol. **A138**, 687-693.

Kittler M, Seifert W (1993b) Two classes of defect recombination behaviour in silicon as studied by SEM-EBIC. Scanning **15**, 316 -321.

Kittler M, Seifert W (1994) Two types of electron-beam-induced current behaviour of misfit dislocations in Si(Ge): Experimental observations and modelling. Mat. Sci. Eng. **B24**, 78-81.

Kittler M, Ulhaq-Bouillet C, Higgs V (1994) Recombination activity of "clean" and contaminated misfit dislocations in Si(Ge) structures. Mat. Sci. Eng. **B24**, 52-55.

Kusanagi S, Sekiguchi T, Sumino K (1992) Difference of the electrical properties of screw and 60° dislocations in silicon as detected with temperature-dependent electron beam induced current technique. Appl. Phys. Lett. **61**, 792-794.

Kveder VV, Ossipiyan Yu A, Schroter W, Zoth G (1982) On the energy spectrum of dislocations in silicon. Phys. Stat. Sol. **A72**, 701-713.

Labusch R, Schroter W (1978) Electrical properties of dislocations in semiconductors. In: Dislocations in Solids. Vol. 5. Nabarro FRN (ed.). North-Holland, Amsterdam. pp. 127-191.

Lester SD, Ponce FA, Craford MG, Steigerwald DA (1995) High dislocation densities in high efficiency GaN-based light-emitting diodes. Appl. Phys. Lett. **66**, 1249-1251.

Lesniak M, Holt DB (1983) Electrically active defects in Si photodetector devices. In: Microscopy of Semiconducting Materials 1987. Inst. Phys. (Bristol) Conf. Series No. 67. pp. 439-444.

Lesniak M, Holt DB (1987) Defect microstructure and microplasmas in silicon avalanche photodiodes. J. Mater. Sci. **22**, 3547 -3555.

Logan RA, Pearson GL, Kleinman DA (1959) Anisotropic mobilities in plastically deformed germanium. J. Appl. Phys. **30**, 885-895.

Lohnert K, Kubalek E (1983) Characterization of semiconducting materials and devices by EBIC and CL techniques. In: Microscopy of Semiconducting Materials 1983. Inst. Phys. (Bristol) Conf. Series No. 67. pp. 303-314.

Luo H, Furdyna JK (1995) The II-VI semiconductor blue-green laser: Challenges and solutions. Semicond. Sci. Technol. **10**, 1041-1048.

Maeda K, Takeuchi S (1981) Recombination enhanced dislocation glide in InP single crystals. Appl. Phys. Lett. **42**, 664-666.

Marklund S (1979) Electron states associated with partial dislocations in silicon. Phys. Stat. Sol. **B92**, 83-89.

Masut R, Penchina CM, Farvaque JL (1982) Occupation statistics of dislocation deep levels in III-V compounds. J. Appl. Phys. **53**, 4964-4969.

Matare HF (1955) Korngrenzenstruktur und ladungstragertransport in halbleiterkristallen (Grain boundary structure and charge carrier transport in semiconductor crystals). Z. Naturforsch. **10a**, 640-652.

Matare HF (1956) Korngrenzen-transistoren (Grain boundary transistors). Elektronische Rundschau **8**, 209-255.

Merten L (1964a) Modell einer schraubenversetzung in piezoelektrischen kristallen I. and II (Model of a screw dislocation in piezoelectric crystals I. and II). Physik Kondens. Mat. **2**, 53-79.

Merten L (1964b) Piezoelektrische potentialfelder um stufenversetzungen belibiger richtung in piezoelektrischen kristallen mit elastischer isotropie (Piezoelectric potential fields of edge dislocations in piezoelectric crystals with elastic isotropy). Z. Naturforsch. **19a**, 1161-1169.

Morrison SR (1956) Recombination of electrons and holes at dislocations. Phys. Rev. **104**, 619-623.

Mueller RK (1959) Transient response of grain boundaries and its application for a novel light sensor. J. Appl. Phys. **30**, 1004-1010.

Mueller RK, Jacobson RL (1959) Grain boundary photovoltaic cell. J. Appl. Phys. **30**, 121-122.

Neubert D, Kos J, Hahn D (1973) Problems of lifetime doping by dislocation in silicon. In: Solid State Devices 1972. Inst. Phys. (London, now in Bristol) Conf. Series No. 15. 220 (abstract).

Neumark GF, Park RM, DePuydt JM (1994) Blue-green diode lasers. Physics Today (June), 26-32.

Newman R (1955) Visible light from a silicon p-n junction. Phys. Rev. **100**, 700-703.

Ogden R, Wilkinson JM (1977) Characterization of crystal defects at leakage sites in charge-coupled

devices. J. Appl. Phys. **45**, 412-414.

Omling P, Weber ER, Montelius L, Alexander H, Michel J (1985) Electrical properties and point defects in plastically deformed silicon. Phys. Rev. **B32**, 6571-6581.

Ono H, Sumino K (1985) Defect states in p-type silicon crystals induced by plastic deformation. J. Appl. Phys. **57**, 287-292.

Ossipiyan Yu A (1981) Dislocation microwave electrical conductivity of semiconductors and electron-dislocation spectrum. Cryst. Res. Technol. **16**, 239-246.

Ossipiyan Yu A (1983) Dislocation electron spectrum and the mechanism of dislocation microwave conduction in semiconductors. J. de Phys. Colloque **C4**, 103-111.

Ourmazd A, Wilshaw PR, Booker GR (1983) The temperature dependence of EBIC contrast from individual dislocations in silicon. J. de Phys. Colloque **C4**, 289-295.

Parekh PC (1971) The influence of stationary dislocations and stacking faults on some transistor parameters. Sol. State Electron. **14**, 273-280.

Pasemann L (1981) A contribution to the theory of the EBIC contrast of lattice defects in semiconductors. Ultramicroscopy **6**, 237-250.

Pasemann L, Hergert W (1986) A theoretical study of the determination of the depth of a dislocation by combined use of EBIC and CL technique. Ultramicroscopy **19**, 15-22.

Pearson GL, Riesz RP (1959) High-speed switching diodes from plastically deformed germanium. J. Appl. Phys. **30**, 311-312.

Petroff PM, Hartman RL (1973) Defect structure introduced during operation of heterojunction GaAs lasers. Appl. Phys. Lett. **23**, 469-471.

Petroff PM, Hartman RL (1974) Rapid degradation phenomenon in heterojunction GaAlAs-GaAs lasers. J. Appl. Phys. **45**, 3899-3903.

Petroff PM, Lang DV (1977) A new spectroscopic technique for imaging the spatial distribution of nonradiative defects in a scanning transmission electron microscope. Appl. Phys. Lett. **77**, 60-62.

Petroff PM, Lorimer OG, Ralston JM (1976) Defect structure induced during forward-bias degradation of GaP green-light-emitting diodes. J. Appl. Phys. **47**, 1583-1588.

Petroff PM, Lang DV, Strudel JL, Savage A (1978) New STEM spectroscopic techniques for simultaneous electronic analysis and observation of defects in semiconductor materials and devices. Proc. 9th Int. Congr. Electron Microsc., Toronto, 1978, Vol. 1. Microscopical Soc. Canada, Toronto, Canada. pp. 130-131.

Ravi KV, Varker CJ, Volk CE (1973) Electrically active stacking faults in silicon J. Electrochem. Soc. **120**, 533-541.

Raza B, Holt DB (1991) EBIC contrast of grain boundaries in polycrystalline silicon solar cells. In: Polycrystalline Semiconductors II. Werner JH, Strunk HP (eds.). Springer Proc. in Phys. Vol. 54. Springer-Verlag, Berlin. pp. 72-76.

Raza B, Holt DB (1995) EBIC studies of grain boundaries. In: Microscopy of Semiconducting Materials 1995. Inst. Phys. (Bristol) Conf. Series. No. 146 pp. 107-112.

Read WT (1954a) Theory of dislocations in germanium. Phil. Mag. **45**, 775-796.

Read WT (1954b) Statistics of the occupation of dislocation acceptor centers. Phil. Mag. **45**, 1119-1128.

Read WT (1955) Scattering of electrons by charged dislocations in semiconductors. Phil. Mag. **46**, 111-131.

Rodzimski ZJ, Zhou TQ, Buczkowski AB, Rozgonyi GA, (1991) Electrical activity of dislocations-prospects for utilization. Appl. Phys. A. Sol. Surf. **53**, 189-193.

Roedel RJ, Von Neida AR, Caruso R (1979) The effect of dislocations in $Ga_{1-x}Al_xAs$:Si light-emitting diodes. J. Electrochem. Soc. **126**, 637-641.

Ross FM, Hull R, Bahnck D, Bean, JC, Peticolas LJ, King CA (1993a) Changes in electrical device characteristics during the *in situ* formation of dislocations. Appl. Phys. Lett. **62**, 1426-1428.

Ross FM, Hull R, Bahnck D, Bean JC, Peticolas LJ, King CA, Kola RR (1993b) Changes in electrical device characteristics during the formation of dislocations *in situ* in the TEM. In: Microscopy of Semiconducting Materials 1993. Inst. Phys. (Bristol) Conf. Series No. 134. pp. 245-248.

Roy K (1971) Relationship between hot-spots and growth defects in epitaxially grown p-n junctions. J. Cryst. Growth **9**, 139-143.

Rozgonyi GA, Salih ASM, Radzimski ZJ, Kola RR, Honeycutt J, Bean KE, Lindberg K (1987) Defect engineering for VLSI epitaxial silicon. J. Crystal Growth **85**, 300-307.

Sauer R, Weber J, Stolz J, Weber ER, Kuslers KH, Alexander H (1985) Dislocation-related photoluminescence in silicon. Appl. Phys. **A36**, 1-13.

Schroter W, Scheibe E, Schoen H (1980) Energy spectra of dislocations in silicon and germanium. J. Microsc. **118**, 23-34.

Schroter W, Queisser I, Kronewitz J (1989) Capacitance transient spectroscopy of dislocations in semiconductors. In: Structure and Properties of Dislocations in Semiconductors 1989. Inst. Phys. (Bristol) Conf. Series. No. 104. pp. 75-84.

Schumann PA, Rideout AJ (1964) Reduction of the

turn-off delay of a germanium npn mesa by plastic deformation. Sol. State Electron. **7**, 849-851.

Schwuttke GH (1970) Silicon material problems in semiconductor device technology. Microelectron. Reliability **9**, 397-412.

Shockley W (1953) Dislocations and edge states in the diamond crystal structure. Phys. Rev. **91**, 228.

Shockley W (1961) Problems related to p-n junctions in silicon. Sol. State Electron. **2**, 35-67.

Ueda O (1988) Degradation of III-V opto-electronic devices. J. Electrochem. Soc. **135**, 11C-22C.

Weber J (1994) Correlation of structural and electronic properties from dislocations in semiconductors. In: Polycrystalline Semiconductors III. Strunk HP, Werner JH, Fortin B, Bonnaud O (eds.). Scitec Publ., Zurich, Switzerland. pp. 13-24.

Weber ER, Alexander H (1979) EPR of dislocations in silicon. J. de Phys. Colloque **C6**, 101-106.

Weber ER, Alexander H (1983) Deep level defects in plastically deformed silicon. J. de Phys. Colloque **C4**, 319-328.

Wertheim GK, Pearson GL (1957) Recombination in plastically deformed germanium. Phys. Rev. **107**, 694-698.

Wessel K, Alexander H (1977) On the mobility of partial dislocations in silicon. Phil. Mag. **35**, 1523-1536.

Wilshaw PR, Booker GR (1985) New results and an interpretation for SEM EBIC contrast arising from individual dislocations in silicon. In: Microscopy of Semiconducting Materials 1985. Inst. Phys. (Bristol) Conf. Series No. 76. pp. 329-336.

Wilshaw PR, Booker GR (1987) The theory of recombination at dislocations in silicon and an interpretation of EBIC results in terms of fundamental dislocation parameters. Bull. Acad. Sci. USSR Phys. **51**, 109-113.

Wilshaw PR, Fell TS (1989) The electronic properties of dislocations in silicon. In: Structure and Properties of Dislocations in Semiconductors 1989. Inst. Phys. (Bristol) Conf. Series No. 104. pp. 85-89.

Wilshaw PR, Fell TS (1991) The electrical activity of dislocations in the presence of transition metal contaminants in polycrystalline semiconductors II. Werner JH, Strunk HP (eds.). Springer-Verlag, Berlin. pp. 77-83.

Wilshaw PR, Ourmazd A, Booker GR (1983) Some aspects of measurements of electrical effects of dislocations in silicon using a computerized EBIC system. J. de Phys. Colloque **C4**, 445-450.

Wilshaw PR, Fell TS, Booker GR (1989) Recombination at dislocations in silicon and gallium arsenide. In: Point and Extended Defects in Semiconductors. Benedek G, Cavallini A, Schroter W, (eds.). Plenum Press, New York. pp. 243-256.

Wilshaw PR, Fell TS, Coteau MD (1991) EBIC contrast of defects in semiconductors. J. de Phys. Colloque **C6**, 3-14.

Yamakoshi S, Abe M, Wada O, Komiya S, Sakurai T (1981) Reliability of high radiance InGaAsP/InP LED's operating in the 1.2-1.3 μm wavelength. IEEE J. Quantum Electron. **QE-17**, 167-173.

Yu KK, Jordan AG, Longini R (1967) Relations between electrical noise and dislocations in silicon. J. Appl. Phys. **38**, 572-583.

Zipfel CL, Chin AK, DiGiuseppe MA (1983) Reliability of InGaAsP light emitting diodes at high current density. IEEE Trans. Elec. Device Lett. **ED-30**, 310-316.

Discussion with Reviewers

M. Kittler and W. Seifert: According to our detailed studies of misfit dislocations, "clean" dislocations show type-2 behaviour and contamination causes a change from type 2 to type 1 [3]. Consequently, we suggest that these deformation-induced type-2 dislocations are relatively clean, whereas the deformation-induced type-1 dislocations reported by Wilshaw (e.g., [1]) are likely to be surrounded by a point-defect/impurity atmosphere. How do you interpret these observations? Do you think that the point defect atmosphere is an argument against the existence of a space charge cylinder?

Author: Your work is interesting, but the work of Kusanagi *et al.* (1992) shows that the contrast properties for dislocations produced by the Wessel and Alexander (1977) two-temperature deformation technique depend strongly on core geometry, i.e., the behavior of 60° and screw portions of the same hexagonal loop they found to be quite different. Similarly, your parallel misfit dislocations in Figure 10, despite presumably having the same core geometry (60° or pure edge?) and impurity decoration behave very differently. Thus, it appears that, despite all the important recent progress, there are still things that are difficult to explain, and class 1 versus class 2 behaviour is one of them.

M. Kittler and W. Seifert: Band bending due to the dislocation line charge, although significant under equilibrium (dark) conditions, may be lower under electron beam excitation. Furthermore, if one assumes an atmosphere of centers rather than a line charge at the core, band bendings can be low even in equilibrium.

Author: What you say is certainly true, but whether either or both factors together reduce the band bending to a negligible value compared to kT is not clear, and I am inclined to doubt it.

M. Kittler and W. Seifert: The SRH model in its present state applied by us does not pretend to give a really quantitative description. However, it qualitatively describes both the temperature and injection dependant contrast behaviour of type-1 and of type-2 dislocations in Si. This model can also explain experimental C(T) data of dislocations in Si as measured by Wilshaw *et al.* (e.g., Fig. 3 in [5]), showing a temperature dependence in the form of $C \propto (T)^{1/2}$) which were originally taken as a proof of the CCR model. On the contrary, the CCR model does not allow a reliable interpretation of dislocations exhibiting steep contrast increase in the low temperature range (type-2 behaviour). Can you suggest other mechanisms than those considered in SRH theory to explain this behaviour?

Author: No, I cannot suggest any other model to account for the two forms of C(T) behaviour, and the fact that your SRH approach can do so, at least qualitatively, is clearly its main attraction.

V. Higgs: A comment about the nature of the recombination mechanisms: is the CCR theory more applicable to impurity controlled recombination, that is contaminated dislocations, and the SRH theory more representative of the recombination properties of dislocations that are "cleaner"?

Author: That would certainly seem to be the conclusion to be drawn from your own important work. The snag is that as usual, it is more complicated than that. Figure 10 shows three dislocations that behave quite differently despite being presumably of the same core type (parallel misfit dislocations) and similarly impurity contaminated as they were formed in the same environment during the same growth heat-treatment regime. The work of Kusanagi *et al.* (1992) provides further evidence of differences of behaviour that are difficult to ascribe to differences of impurity contamination.

V. Higgs: In light of the role of impurities on dislocation activity, are clean dislocations inactive?

Author: Unfortunately, we have to recognize at least two types of contamination effects. These are passivation, i.e., the decrease of EBIC contrast, etc., due to, for example, hydrogen contamination of dislocations and grain boundaries in silicon and activation, i.e., the increase of EBIC contrast and related properties due to heavy metal contamination as proved by the work of yourself and your coworkers. What the effects of the two types of "benign and malignant" contaminant are in inducing either class 1, class 2 or no-contrast behaviour at various concentrations, I would dearly love to know, but I have no real idea.

In addition, although I hate to suggest it, we might actually sometimes get a combination of passivation and activation resulting in a "U" shaped curve of EBIC contrast against concentration of the impurity or impurities. This could occur due, for example, to fast diffusion of a few hydrogen atoms to a dislocation, followed by slower diffusion of more numerous heavy metal atoms producing first passivation followed by (re)activation. Thus, again, there is much we still do not understand. However, as I often tell discouraged students, this isn't a disaster, it's a career opportunity!